FILE COPY DO NOT CIRCULATE

FOR USE OF G-E EMPLOYEES ONLY

GENERAL ELECTRIC

TECHNICAL INFORMATION SERIES

Title Page

AUTHOR	SUBJECT CLASSIFICATION	NO.
W. D. Simpson	Failure Analysis	66SD281
		DATE: August 6, 1966

TITLE

FINAL REPORT - FAILURE ANALYSIS AND DESIGN REPORT OF NIMBUS I SOLAR ARRAY DRIVE FAILURE

ABSTRACT

The Nimbus I Weather Satellite failure was investigated by analysis and laboratory tests. The failure was found to be due to deterioration of the grease in the Solar Array Drive motor bearings due to high (>300F) temperature conditions. Corrective design changes lowered temperatures to less than 200F; subsequent laboratory and flight tests have been successful.

G.E. CLASS	REPRODUCIBLE COPY FILED AT	NO. PAGES
II	MSD Documents Library;Valley Forge STC;PO Box 8555; Phila.,Pa. 19101	63
GOV. CLASS. Unclassified		

CONCLUSIONS

1. The Nimbus I flight failure was induced by high temperature(greater than 300F) conditions in the Solar Array Drive Motor bearings. The high temperatures caused deterioration of the G300 silicone grease lubricant,increasing motor bearing friction and producing motor stall.
2. The high temperature condition was a design and operating characteristic and was not caused by variabilities or anomalies.
3. The design and operation of the Solar Array Drive has been modified to reduce maximum temperature well within that required for reliable, long-life operation(less than 200F).

By cutting out this rectangle and folding on the center line, the above information can be fitted into a standard card file.

For list of contents—drawings, photos, etc., and for distribution see next page (FN-610-2).

INFORMATION PREPARED FOR National Aero. & Space Admin., GSFC, Greenbelt, Maryland

TESTS MADE BY L. Gabrovic, P. Lautensack, J. Schwartz, W. Simpson, and others

COUNTERSIGNED Joseph Mintz DIV.

DIVISIONS MSD LOCATION Philadelphia, Pa. 19101

FN-610-1 (1-69)

GENERAL ELECTRIC COMPANY
TECHNICAL INFORMATION SERIES
CONTENTS PAGE

CONTENTS OF REPORT

NO. PAGES TEXT 63

NO. CHARTS

DRAWING NOS.

PHOTO NOS.

DISTRIBUTION

General Electric

M. Berkowitz
H. Raymond
F. Kieser
S. Macklis
P. Lautensack
D. Kirkpatrick
L. Farnham
E. Pelling
I. S. Haas
J. Turtil
R. Barcus
C. W. Whitmore
I. Clausen
S. Drabek
W. Becraft
A. Machuta
E. Buerger
A. Watts
L. Seaman
H. Lazar
D. Bahr, RSD
G. Fox

NASA

H. Press
J. Devlin
J. Sargent
M. Schneebaum
S. Weiland

TABLE OF CONTENTS

ACKNOWLEDGEMENTS AND REFERENCES

In preparing this report, extensive use was made of material which originally appeared in a number of the documents referenced below.

NIMCO SOLAR ARRAY DRIVE: MATERIALS, LUBRICANTS AND LUBRICANT PERFORMANCE DATA (PIR 9381-0352) - 10/14/64 - T. R. Neville

NIMCO SOLAR ARRAY DRIVE: MATERIALS, LUBRICANTS AND LUBRICANT PERFORMANCE DATA (PIR 9381-0352, Rev. A - 12/1/64 - T. R. Neville

ANALYSIS OF TELEMETRY DATA AND MOTOR GEAR PERFORMANCE CHARACTERISTICS TO IMPROVE THE UNDERSTANDING OF THE SOLAR ARRAY DRIVE FAILURE (PIR 4760-SD-2) - 11/5/64 - S. Drabek

NIMBUS GEAR HEAD DRIVE UNITS MANUFACTURED BY KEARFOTT (PIR 4381-JS/CWJ-005) - 11/13/64 - Jack Schwartz/C. W. Jones

E/M COMPONENT STATUS AND HISTORY (PIR 4720-EAB-010) - 12/18/64 - E. Blagus

SOLAR ARRAY DRIVE FAILURE ANALYSIS REPORT (PIR 4720-RB-05) - 11/9/64 - R. Barcus

NIMBUS GEAR HEAD DRIVE UNITS MANUFACTURED BY KEARFOTT (Addendum to PIR 4381-JS-CWJ-005 dated 11/13/64) - 11/18/64 - Jack Schwartz/ C. W. Jones

NIMBUS SOLAR ARRAY DRIVE LUBRICANT INVESTIGATION - 12/14/64 - R. C. Elwell/ W. D. Simpson

COMPARISON OF G-300 WITH ALTERNATE HIGH VACUUM LUBRICANTS (PIR 4371-0035) - 2/4/65 - T. R. Neville/ L. Gabrovic

SOLAR ARRAY DRIVE S/N 4, GE 875D583-G2 (PIR 4381-CWJ/JS-023) - 12/16/64 - C. W. Jones/ Jack Schwartz

POST TEST ANALYSES OF MOTOR GEARHEADS USED IN THE NIMBUS FAILURE VERIFICATION TESTING (PIR 4375-033) - 5/20/65 - L. J. Gabrovic/ R. R. Boileau

ACKNOWLEDGEMENTS AND REFERENCES (Continued)

SOLAR ARRAY DRIVE MOTOR BEARING TEMPERATURE MEASUREMENT TEST REPORT (PIR 4375-030) - 5/14/65 - G. McKinley/ L. Gabrovic/T. Neville/R. Law/H. Wanger/ M. Peucker

FINAL AC SERVO MOTOR #11 THERMAL ANALYSIS (PIR 4142-509) - 5/5/65 - P. E. Jasper

STATIC THIN FILM GREASE EVAPORATION TEST REPORT (PIR 4375-034) - 5/28/65 - T. R. Neville

NIMBUS METEOROLOGICAL SATELLITE - INTEGRATION AND TESTING MATERIALS REPORT NO. 8 (Document 65SD4410) - July, 1965 - T. R. Neville

INTERIM SOLAR ARRAY DRIVE FAILURE ANALYSIS REPORT (PIR 4720-RB-05) 11/9/64 - R. Barcus

1.0 INTRODUCTION

General

The Nimbus I Weather Satellite was launched August 28, 1964. After 26 days of successful operation, Nimbus I prematurely stopped operating due to the failure of the Solar Array Assembly to maintain its proper orientation with respect to the sun. This document summarizes the Failure Analysis and Design Improvement action instituted to resolve this failure.

Contents and Organization

The Nimbus I Flight History, Description and Theory of Operation of the Nimbus I configuration, and the history of the post-flight investigation are included in this section of the report. Summary and Conclusions are given in Section II, followed by a detailed Post-Flight Analysis, Section III. Section IV contains the results of the Failure Verification program; Section V discusses the Design Improvements incorporated for later units; and Section VI cites the Life Assurance Testing accomplished to date.

Flight History

The Nimbus I Weather Satellite was launched August 28, 1964, from the Pacific Missile Range, California, (see Table 1). Initial operation of the vehicle was very successful. During its lifetime, Nimbus I sent back to earth more than 27,000 day and night time photographs showing weather conditions all over the world. Minor operating difficulties were encountered with some of the satellite systems; the Solar Array Drive System operated normally except that after a time it was observed from telemetry data that the control phase voltage continued to increase slowly until after the 300th orbit. The applied voltage then began to fluctuate and to increase more rapidly until on the 354th orbit, saturation voltage was reached and the array stopped tracking the sun. Subsequently, though the array sometimes moved, it did not track the sun until the 358th orbit, when the applied voltage suddenly dropped to near normal and normal tracking resumed. This condition continued until the 372nd orbit when the voltage suddenly saturated at the maximum value again and the array stopped tracking the sun. All array movements stopped after orbit 374 and never resumed.

NIMBUS I LAUNCH DATA

LAUNCH VEHICLE: Thor Agena B

LAUNCH SITE: Pacific Missile Range, California

LAUNCH DATE: August 28, 1964 at 1257 A.M. PDT

ORBIT:

Apogee:	578 Statute Miles
Perigee:	262 Statute Miles
Period:	103.7 Minutes
Inclination:	81 degrees, retrograde

OPERATIONAL LIFETIME:

Approximately 375 orbits, 26 days.
Solar array tracking stopped September 21, 1964.

Table I, Section I

The other Nimbus I systems continued to operate normally until shut-down to conserve power or until the batteries were exhausted. The satellite partially revived for a brief period when the Solar Array paddles were oriented toward the sun by chance shifting of the satellite's tumbling action, but Solar Array Drive operation did not resume.

Description and Operation of the Flight Configuration

Nimbus Vehicle

The Nimbus I spacecraft configuration is shown in Figure 1.

The Sensory Ring Assembly contains the picture-taking and conditioning equipment comprising the payload, plus other auxiliary equipment. The Controls Subsystem Assembly contains the attitude control, power and related equipments; it is physically packaged as a separate unit and is joined to the Sensory Ring Assembly by a truss structure. Two Solar Cell Array Paddle assemblies for the collection of solar energy are mounted to the output shaft of the Control Subsystem assembly, one on each side of the spacecraft.

Controls Subsystem Assembly

The Controls Subsystem Assembly configuration is shown in Figure 2. The structure is in the form of a hexagonal cylinder, with attached external box structures containing horizon scanners and amplifiers. Internally, the assembly is radially partitioned, providing package rigidity and mounting spaces for the attitude control equipment and the Solar Array Drive Subsystem equipment. The shaft to which the Solar Array Paddles are mounted extends completely through the Control box assembly and is hollow to allow passage of electrical power and sensing leads from the paddles. Two large diameter ball bearings attached to outer panels of the hexagonal structure support the paddle shaft. The Solar Array Drive Assembly and the Slip Ring Assembly have short, hollow shafts through which the paddle drive shaft passes and to which it is then attached by locking pins.

The mounting and description of other systems and components such as the electronics, momentum wheels, and gyro will not be discussed in this report.

Solar Array Drive Assembly

The Nimbus I Solar Array Drive Assembly Configuration is shown in Figures 3, 4, and 5. The assembly consists of a motor gearhead unit, a potentiometer unit, and a sub-assembly unit containing a clutch, output shaft, and gearing. The motor of the motor gearhead unit is a Size 8, two-phase AC Servo motor; it drives a 12000:1 spur gear train in the gearhead section. All bearings and gear meshes of the motor gearhead are lubricated at assembly with G-300 silicone grease. A nylasint reservoir in the motor cover is impregnated at assembly with F50 silicone oil. The output gear of the motor-gearhead drives a 7:1 spur gear reduction train in the housing sub-assembly unit and connected to the output shaft. A ball-detent face clutch is provided in this gear train to protect the motor gearhead from injury by back-driving from the shaft end. All parts in this sub-assembly are lubricated with G-300 silicone grease and a nylasint reservoir is impregnated with F50 silicone oil. The potentiometer unit mounts on to the housing sub-assembly and contains four wire-wound potentiometer cups. It is driven by a 1:1 gear train from the output shaft independent of the clutch. The potentiometer bearings are lubricated with G-300 grease; the wiper and windings are unlubricated noble metals. Design data of the Solar Array Drive are tabulated in Figure 6.

THEORY OF OPERATION

Launch and Acquisition

The Nimbus Spacecrafts are launched from the Pacific Missile Range (PMR) in a polar orbit. The launch vehicle is a two-stage Thor-Agena rocket. Injection into the orbit path occurs at a South latitude over the southwestern part of Madagascar at the end of the second Agena rocket burn.

After injection, twelve seconds is allowed for the Agena to stabilize. Then a one degree per second pitch-up maneuver is initiated and maintained for 80 seconds. The Agena is stabilized at a pitch attitude of ten degrees from the vertical and maintained for twenty seconds. Separation is then initiated by severing the clamp holding the Nimbus Spacecraft to the adapter section affixed to the Agena rocket. Compressed springs impart a separation velocity of four feet per second between the spacecraft and the rocket assuring diverging orbits.

The spacecraft mechanically senses separation and after 2.5 seconds the paddle unfold mechanism is activated and the reset-separate relay is switched to the separate condition to activate the controls subsystem programmer.

At separation the vehicle is nominally in an orbit path which is circular at an altitude of 500 to 600 nautical miles. (Nimbus I orbit was eccentric, see Table I).

The orbit is inclined at an angle of approximately 81 degrees from the equator so that the regression of the nodes of the orbit plane about the equator nearly match the rotational movement of the earth about the sun. The purpose of maintaining the orbit plane of the spacecraft at all times parallel to a line between the earth and the sun is to reduce to one axis of motion the requirement for maintaining the spacecraft solar paddles perpendicular to the sun.

The period of the nominal orbit is slightly over 100 minutes with approximately one-third of this time (35 minutes) spent passing through the earth's umbra. Spacecraft sunset occurs in the northern hemisphere and sunrise in the southern hemisphere. (Nimbus I period was approximately 104 minutes).

Following separation from the launch vehicle, the Control Subsystem stabilizes the satellite, i.e., aligns the body axes with the orbit axes within two orbits after separation. Nominally, stabilization occurs within the first quarter orbit. Following initial stabilization, the Control Subsystem maintains stabilized attitude, i.e., the yaw axis must point to the earth and the roll

axis must be in the orbit plane. Pointing accuracy about all axes is maintained to within one degree. The instantaneous angular rate of the satellite body axes relative to the orbit axes is less than 0.05 degree per second. Maintaining this stabilization is required for the sensory ring equipment to operate properly.

Solar Array Control Subsystem

The Solar Array Subsystem block diagram is shown in Figure 7. The subsystem consists of two sun sensor assemblies mounted on the Solar Array paddle; associated electronic packages, mounted on the paddle shaft and in the Control Box Assembly; and the Solar Array Drive Assembly, which has been described previously.

The solar array control subsystem maintains the solar array paddles perpendicular to the sun during the daylight portion of the orbit about an axis parallel to the pitch axis. Because the satellite is in a high noon orbit, and the yaw control loop orients the satellite pitch axis normal to the orbital plane which is in the earth-sun plane, the solar array paddles require only single-axis control. The two solar array sun sensors provide error detection. The sun sensors have a cylindrical configuration with solar cells mounted on the surface to provide a 360-degree field of view about the shaft axis. When the solar array paddles are parallel to the sun line, the sun sensors provide maximum output. A preamplifier amplifies the sun sensor signal and supplies the amplified signal as one of two inputs to the drive amplifier. During the dark period of each orbit, the sun sensors produce no signal. At this time, a bias voltage is introduced at the summing point before the drive amplifier by the Sunrise Bias potentiometer output, which is one of the cups of the multi-cup potentiometer unit mechanically linked to the solar array shaft. The output of the potentiometer is a function of shaft position (see Figure 8) and is attenuated by a factor of 50 at the drive amplifier input. The purpose of this potentiometer is to provide a signal to drive the solar array to a preset position during the satellite dark period for rapid sun acquisition when the satellite emerges (sunrise). The potentiometer signal drives the solar array shaft at about five times orbital rate to the stable null position corresponding to satellite sunrise.

During the day period the sun sensor signal overrides the bias signal and drives the solar array to track the sun; however, the bias voltage is of sufficient magnitude to cause the solar array to vary a maximum of 1.7 degrees from sun position. From sunrise to past noon, the solar array lags the sun, i.e., the sunrise bias causes a negative (counter-clockwise) rotation from sun position. During the remainder of the day period, the sunrise bias causes a positive (clockwise) rotation from sun position.

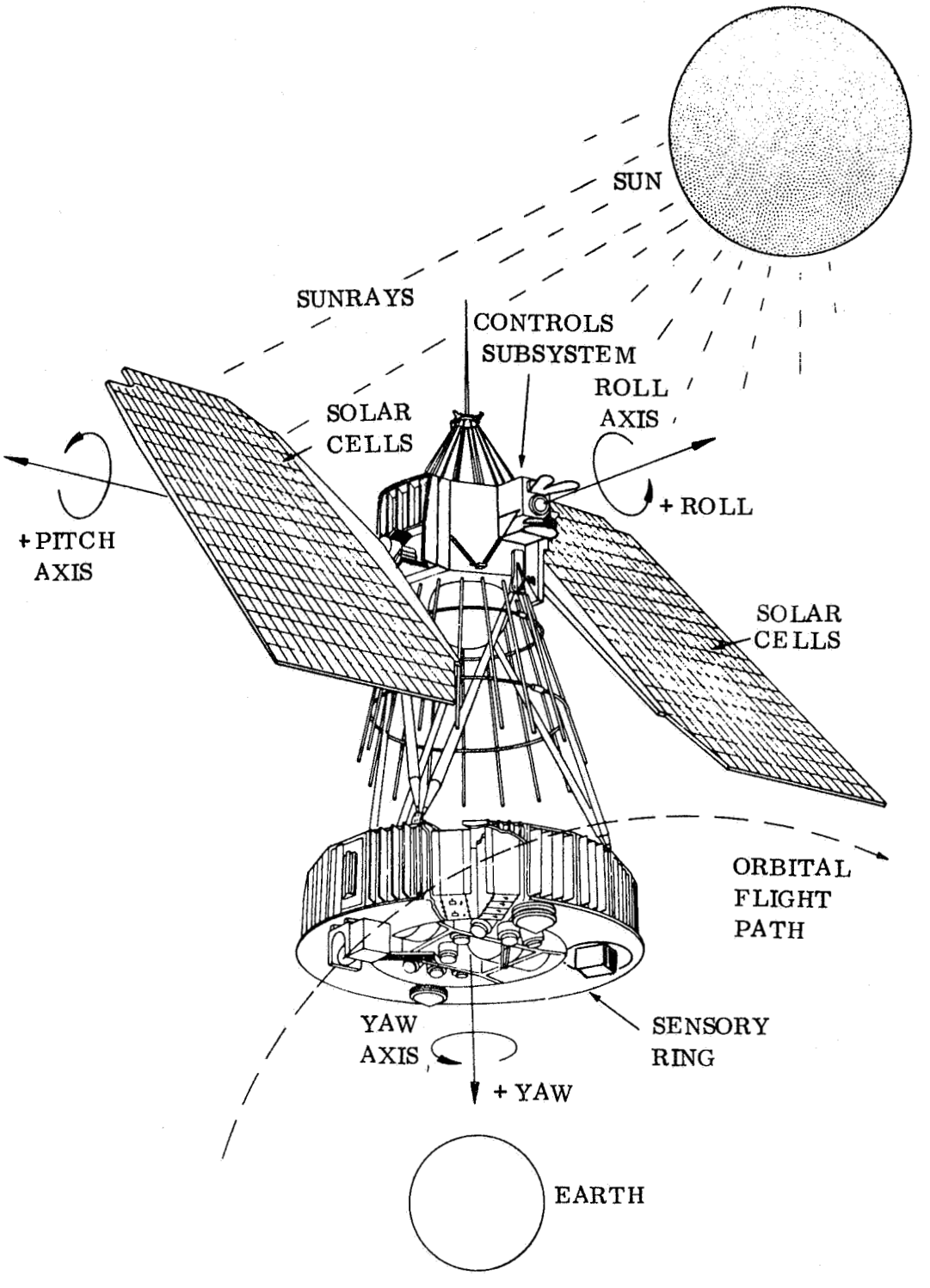

Section 1, Figure 1
Nimbus I Spacecraft Configuration

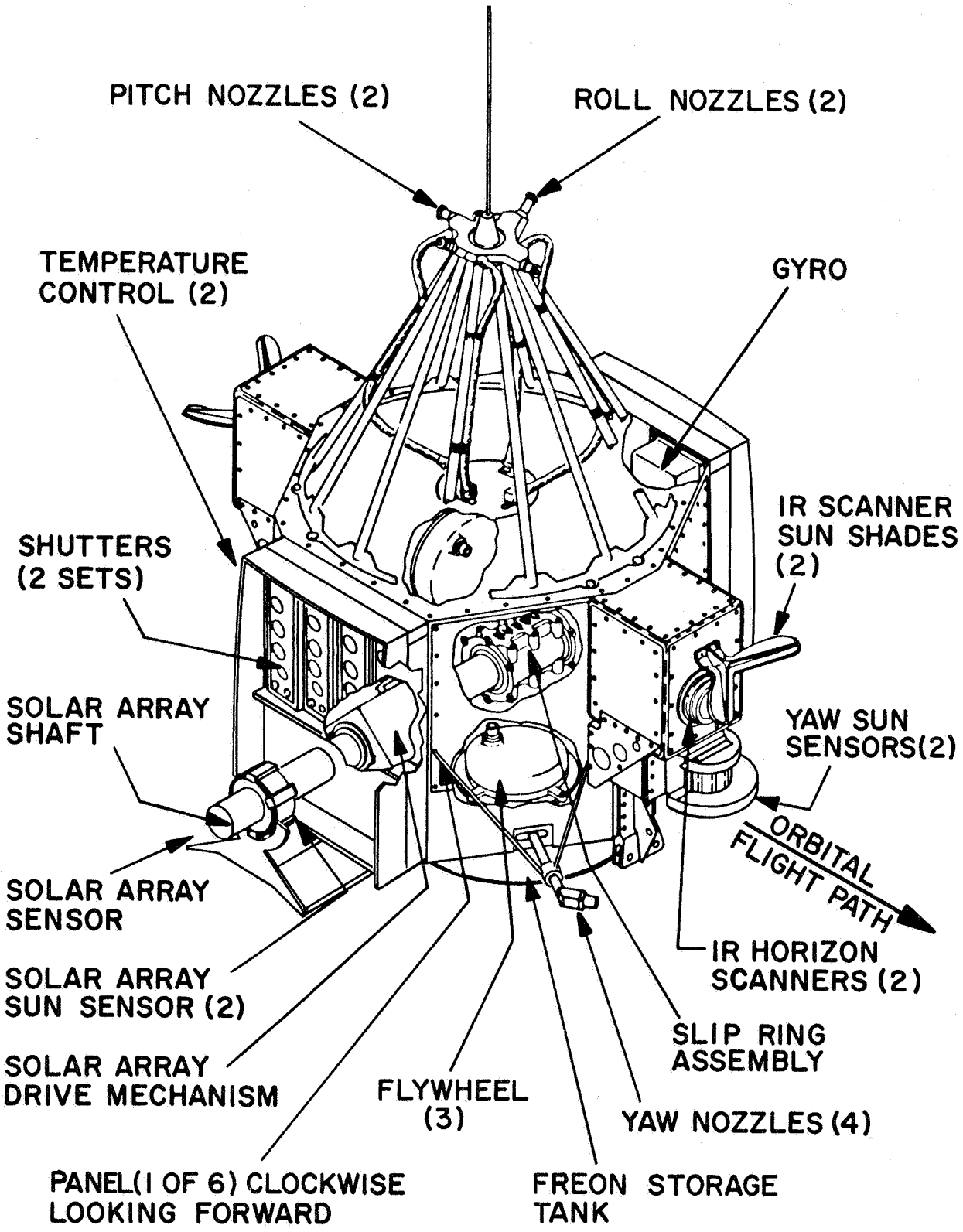

Section 1, Figure 2
Nimbus I Controls Package
Configuration

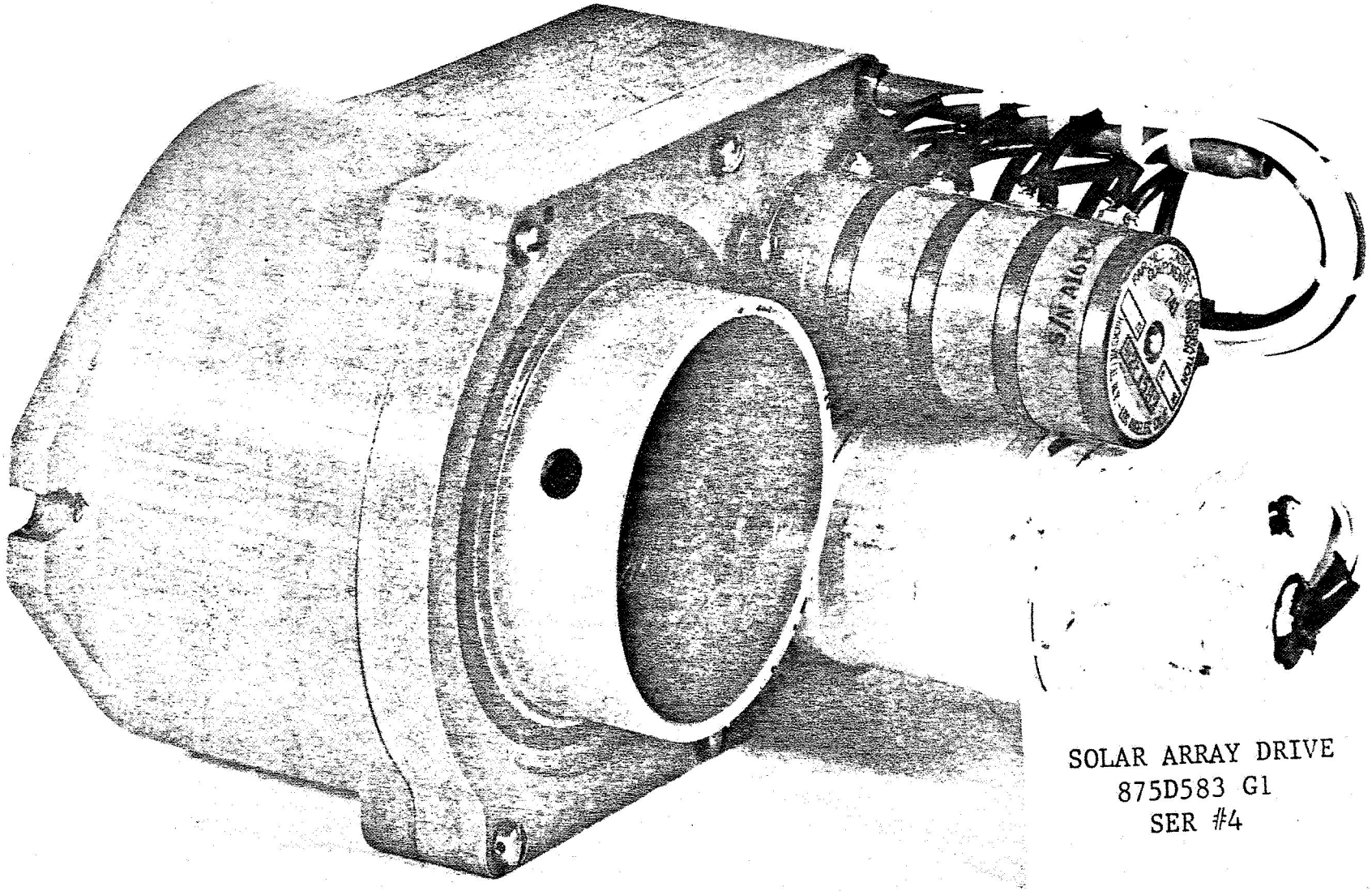

SOLAR ARRAY DRIVE
875D583 G1
SER #4

Section I - Figure 3 "Nimbus I Solar Array Drive"

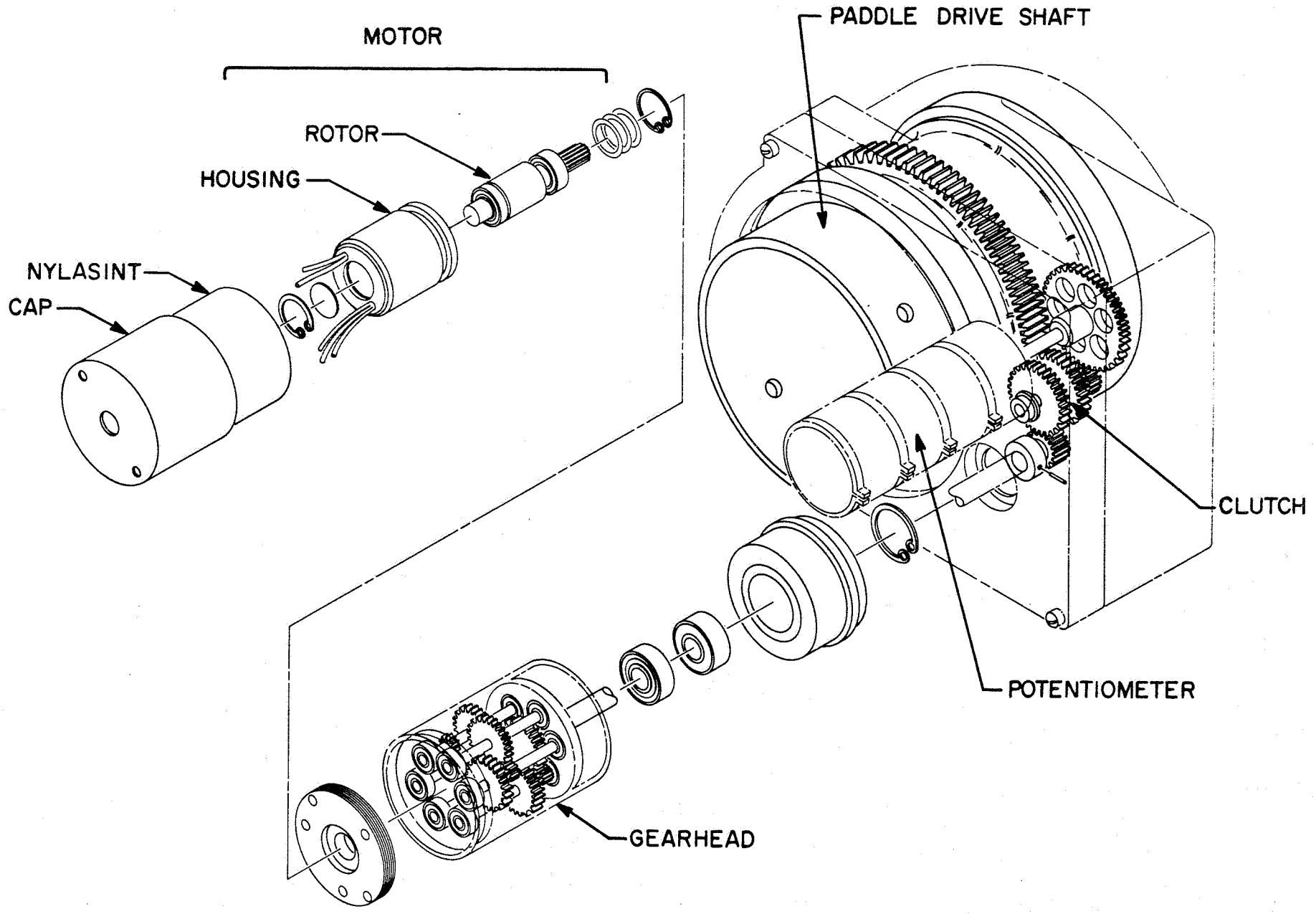

Section 1, Figure 4
Nimbus I Solar Array Drive

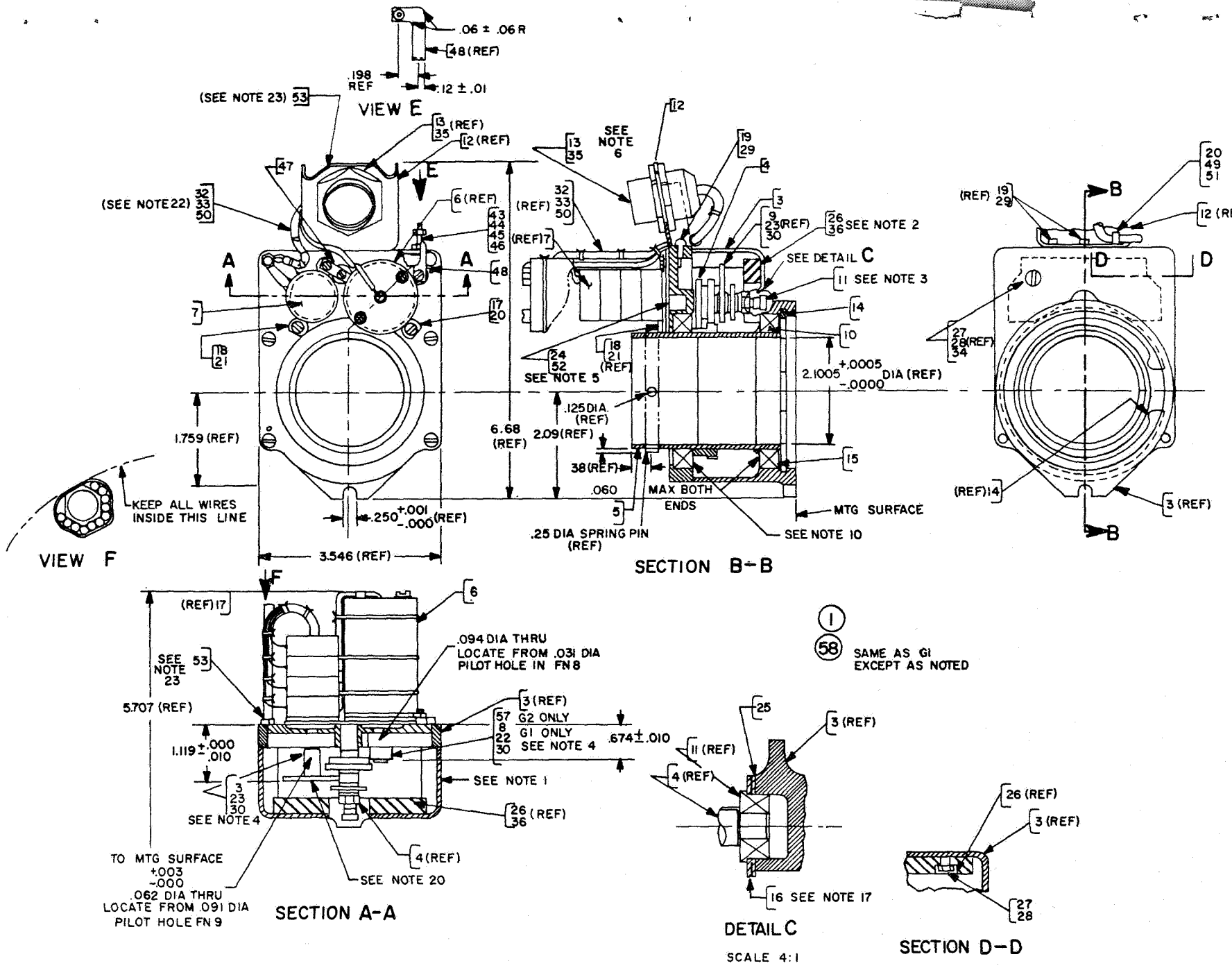

Section 1, Figure 5
Nimbus I Solar Array Drive Assembly

NIMBUS I SOLAR ARRAY DRIVE DESIGN DATA

Motor	2 Ø, 26 VAC, 400 Hertz, Size 8 Servo motor; nominal maximum speed 4500 rpm. Stall torque .10 in. oz. ,minimum.
Gearhead	12,121:1 gear ratio, 7 passes, straight spur gearing.
Clutch	Ball-detent face-type clutch; four stacked Belleville-Washer type springs loading the ball-detent faces. Clutch slip torque 165 in. oz. nominal.
Housing Gearing	All spur gears, 2.33:1 gear ratio before clutch, 3:1 gear ratio after clutch.
Assembly	84,847:1 overall gear ratio. Nominal output torque 495 in. oz. Normal anticipated required torque less than 90 in. oz.
Lubrication	General Electric G-300 silicone grease in gears and bearings. Nylasint reservoirs impregnated with F50 oil.
Bearings	R2, R3, R4 sizes; 440C St. Stl. balls and races, crown retainers.

SECTION I FIGURE 6

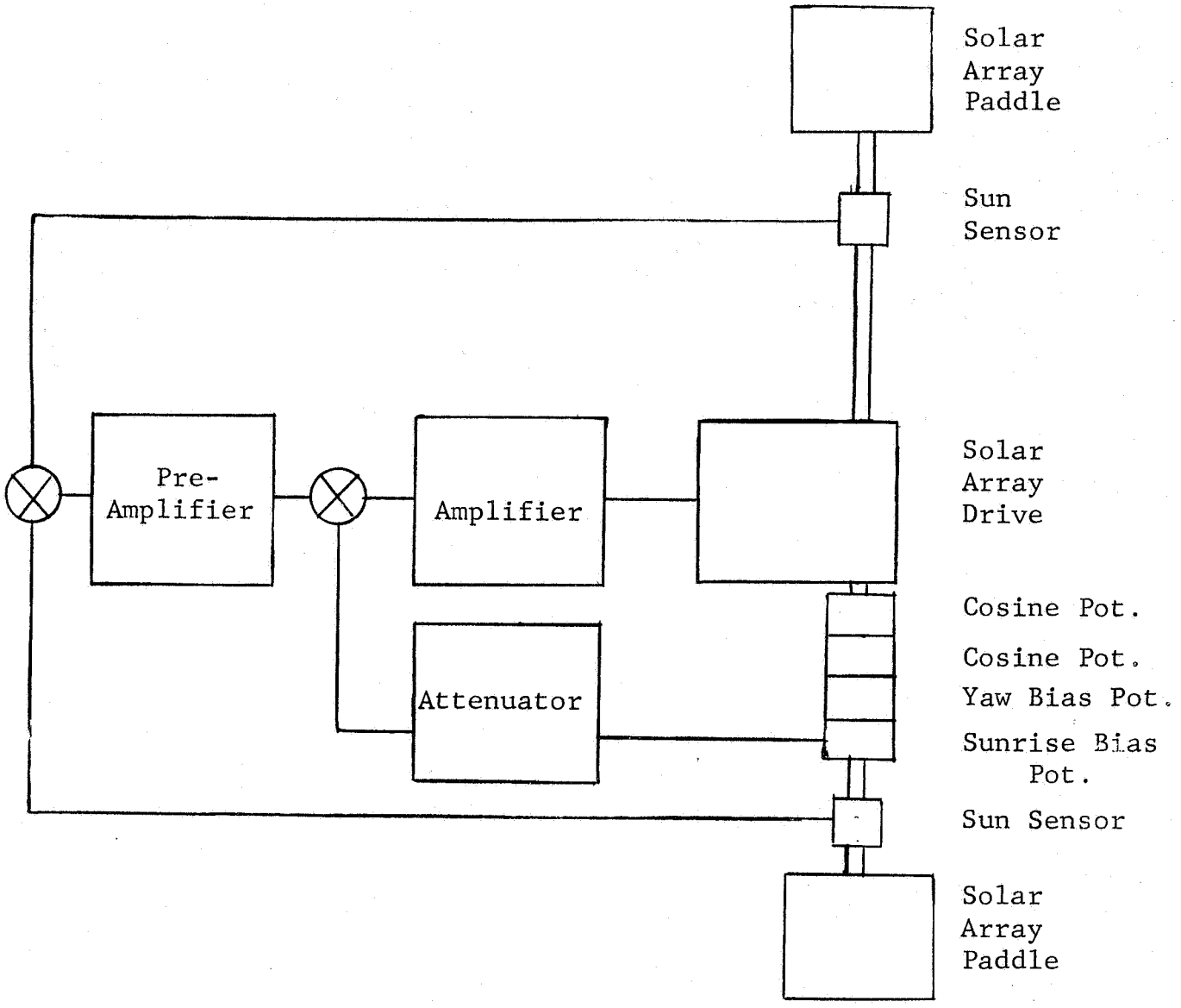

SECTION I FIGURE 7
SOLAR ARRAY SUB SYSTEM - BLOCK DIAGRAM

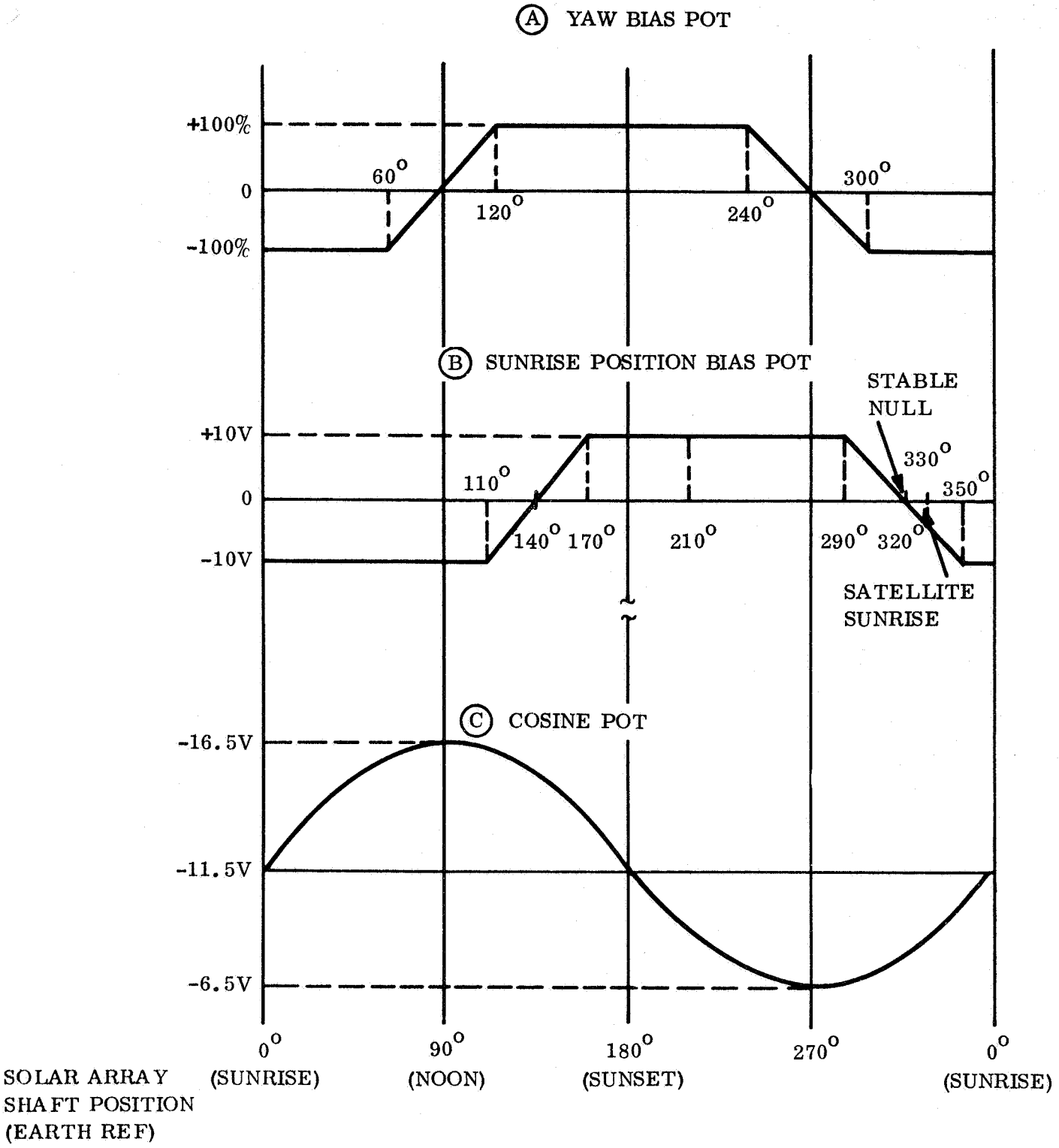

Section 1, Figure 8
Solar Array Drive Potentiometer Schedules

2.0 SUMMARY AND CONCLUSIONS

Summary

The Nimbus I Weather Satellite was launched August 28, 1964. After 26 days of operation Nimbus I prematurely stopped operating due to failure of the Solar Array Assembly to maintain its proper orientation with respect to the sun. An extensive analysis and test program succeeded in pinpointing the cause and duplicating the failure, which was determined to be due to deterioration of the grease in the motor bearings under very high (>300°F) temperature conditions. Corrective design changes, including improved heat transfer and lower input power, has reduced bearing operating temperatures to well under 200°F. Units of the new design have been life-tested in vacuum for more than 6,000 hours. The second Nimbus vehicle, launched May 15, 1966, had exceeded Nimbus I life by thirty days as of August 1, 1966, and was operating normally.

Conclusions

1. The Nimbus I flight failure was induced by high temperature (greater than 300°F) conditions in the Solar Array Drive motor bearings. The high temperatures caused deterioration of the G-300 silicone grease lubricant, increasing motor bearing friction and producing motor stall.

2. The high temperature conditions was a design and operating characteristic and was not caused by variabilities or anomalies.

3. The design and operation of the Solar Array Drive has been modified to reduce maximum temperature well within that required for reliable, long-life operation (less than 200°F).

Recommendations

1. It is recommended that all complex electro-mechanical devices be life-tested under simulated orbital conditions and with suitable instrumentation to detect incipient failure trends. The worth of such testing far outweighs the cost when it reveals deficiencies which would cause flight failures. The probability of unknown deficiencies in complex electro-mechanical units is relatively very high due to the great many parameters which affect the operation of these devices.

3.0 POST-FLIGHT ANALYSIS

Introduction

Subsequent to the flight failure, an extensive analysis of the telemetry data and of all elements of the spacecraft Solar Array Subsystem was made. The investigation included review of possible failure modes, materials, specifications, requirements, and test history. Special tests were conducted to check possible failure mode theories.

Post-Flight Analysis Conclusions

It was tentatively concluded that the flight failure was caused by a failure in the motor gearhead unit of the Solar Array Drive assembly. The failure appeared to be due to lack of lubrication or to contamination.

Analysis of Flight Data

An orbit-by-orbit examination of the telemetered flight data was made to establish the failure signature. Of the data telemetered, three channels proved to have information relative to the Solar Array Drive failure.

A. Solar Array Drive Amplifier Output -- This is a DC signal, 0 to -6.4 volts, formed by rectification of the AC motor drive signal. The actual circuit is shown in Figure 1. The telemetry calibration for this signal is shown in Figure 2. Data is sampled once a frame (16.2 seconds).

B. Cosine Pot Output -- This signal is used primarily for iris control of the AVCS. It is telemetered and is useful as a measure of shaft rotation position. Because it is a cosine function, the signal position gain is very low over large portions of the shaft position range. The telemetry calibration for this signal is shown in Figure 3. Data is sampled once a second.

C. Unregulated Bus Current -- This signal is proportional to the bus current directly off the paddles and is a function of the cell current output versus source angle of incidence to the cell surface. This signal provides a qualitative assessment of paddle tracking error during portions of an orbit. It is affected by attitude errors of the vehicle about all three axes at various portions of the orbit and therefore must be used cautiously. It does give an indication of entry into umbra, which is useful reference point in assessing the other data. Its telemetry calibration is shown in Figure 4. Data is sampled once every 16.2 seconds.

Special print-outs of these traces side by side were made for analysis. A sample of an early orbit is shown in Figure 5. Referring to Figure 5, the data shown are typical of the first 200 orbits. Time progresses from the bottom of the sheet toward the top as the satellite orbits the Earth. During the satellite "day", the unregulated bus current remains at almost a constant value as the solar array is kept oriented toward the sun; the input control voltage to the Solar Array Drive stays within a relatively narrow band except for several short intervals which will be explained below. Meanwhile, the cosine potentiometer output decreases slowly indicating the rotational position of the solar array shaft.

At satellite sunset, the unregulated bus current drops to zero since the solar cells do not receive energy from the sun and simultaneously the input voltage to the Solar Array Drive increases to saturated value as the sun sensor output is cut off and the feedback potentiometer bias voltage takes effect. The Solar Array Drive immediately speeds up to approximately five times orbit rate and drives the solar paddles to the approximate sunrise position. At this point the input voltage reduces to near zero due to the change in bias voltage from the feedback potentiometer as its shaft is turned. The speed increase and subsequent pause in rotation can be verified by observing the variance in the rate of change of the output voltage of the cosine potentiometer.

At sunrise, the unregulated bus current abruptly increases but does not attain its maximum value because the paddles are not quite oriented to the sun-tracking position. The sun sensors immediately detect this and cause the Solar Array Drive input voltage to go to saturation value in order to produce maximum slewing rate and catch up with the sun. This accomplished, the input voltage falls to a steady-state level and the unregulated bus current attains its normal value.

There are several departures from the anticipated normal operation of the spacecraft Solar Array System which need explanation. At points "A" on the drive voltage and cosine potentiometer traces, it can be seen that the drive has reversed direction for a short period and is slewing at a high rate in the opposite direction from that needed to track the sun. (Note that the input voltage trace shows only magnitude, not polarity.) It then reverses and slews rapidly until it once more catches up with the sun and resumes normal tracking. This peculiarity was caused by the fact that Nimbus I was placed in orbit such that there was a slight tilt angle between the orbital plane and the sun line; a corner of the sun shades for the temperature control shutters then projected slightly into the line of sight between the sun and the Solar Array Drive sun sensors just before and after satellite high noon. The resultant shadowing of the sun sensors first on one side only and then on the other side only produced a false indication of the sun position such that the Solar Array Drive reversed and drove the Solar Array backward for a short time until orbital motion of the spacecraft moved the shadow away from the sensors. The system then sensed the error, reversed driving direction, slewed rapidly to the proper position and resumed tracking. A similar effect can be observed at point "B", just before sunset on the Cosine potentiometer trace. Here, the shadowing was caused by the albedo shield and was a more gradual effect. Both of these shadowing effects are readily correctible by altering the shielding (corrective changes were incorporated on Nimbus II).

Other irregularities shown in the traces are due to telemetry signal dropouts, such as at point "C", or possibly electrical noise and have no significance with respect to Solar Array Subsystem operation.

Figure 6 shows the operation of the Solar Array Subsystem 20 orbits before final failure. During the satellite day, the average voltage necessary to track the sun has risen from the early value of about 1.5 volts (TM) to about 6.3 volts (TM) and is quite erratic. This effect is very pronounced at the pre- and post-noon shadowing. (Note the change in scale between Figure 5 and Figure 6.)

At night, it takes much longer to drive the solar array to the sunrise position. The high tracking voltage and low speed at saturated voltage could be indicative of a high friction or binding load being seen by the Solar Array Drive motor.

Figures 7 and 8 show an orbit-by-orbit history of the Solar Array Drive input voltage. Certain trends in input voltage during each orbit are evident. From the first orbits after launch, the tracking voltage required gradually rose from sunrise to sunset, but remained at a low value. After the first two hundred orbits, the average tracking voltage per orbit gradually rose until at a few orbits before the first paddle stoppage, the voltage started to rise at an increasing rate each orbit. The drive moved at less than orbital rate for two orbits (354, 355) and stopped completely for two orbits (356, 357). During the orbits when the array was stopped, a few intervals of motion were noticed during the umbra portions of the orbit in the form of short duration fast movements through arcs of a few degrees.

The minimum voltage attained during each dark period when the array drives to the dark period null is a measure of the frictional torques that exist in the drive as reflected back to the motor rotor. This voltage history indicates erratic frictional forces starting about orbit 320 and markedly increasing friction levels starting at orbit 350. Likewise, this voltage indicates a frictional force which decreased rapidly following orbit 358 until the array jammed in orbit 372.

During the twenty orbits before the first stoppage, a noticeable trend to higher tracking voltages following most motor reversals can be noted. Typical orbits are 338, 343, 345, 349, 352. The change in tracking voltage after a mechanical reversal would appear to be highly significant and perhaps indicative of mechanical, rather than electrical phenomena. When the array again started to drive on orbit 358, the drive voltage dropped immediately to about six volts RMS, but remained very erratic for two orbits before it smoothed out.

The final failure occurred as a sudden lock-up of the drive during a motor reversal.

Failure Mode Analysis

In order to analyze the data to try to determine probable cause and the sequence of the flight failure, a list of possible failure modes of the subsystem and components which could cause stoppag or slow-down of the subsystem was compiled. These failure modes were then analyzed or investigated by testing to evaluate their probability as the cause of the flight failure. The following paragraphs summarize the results of this work.

Possible Solar Array Subsystem and Component Failure Modes

A. Electrical Failure of Amplifier

Temperature build-up in amplifier causing one side of push-pull output to cut off or operate at reduced current output.

A short across output transistor

An open in output transistor

B. Electrical Failure of the Motor

Full voltage not applied to control winding, high resistance in series with field.

Low voltage on fixed phases.

Open motor winding

Shorted motor winding.

C. Mechanical Failure of Motor

High friction on motor bearings or drag on armature due to lubricant loss or gumming.

Mechanical interference due to friction caused by foreign particles in motor (can be intermittent type failure).

D. Mechanical Failure of Gearhead

Friction build-up at input due to loss of lubricant or gumming of lubricant in bearings.

Intermittent friction build-up due to particle interference in bearings.

"High spot" type failure, tendency of gearhead to stick due to high friction at certain positions of output shaft.

Wear of gears, until gears no longer mesh.

E. Clutch Failure

Relaxing of spring tension causing detent torque to drop to nominal value near normal operating torque level. (However, the residual torque between detents would also be reduced to below driving torque level)

Binding of clutch-driven shaft bearings causing failure of pinion gear or clutch-driven gear or internal failure of gearhead.

Binding caused by intermittent jamming by foreign particles.

F. Potentiometer Shaft Binding

Binding of the potentiometer shaft bearings, causing slipping of the clutch.

G. Paddle Shaft Bearing Failure

Increased drag caused by end bearing misalignment due to temperature distortions of structure.

Lubricant gummed up -- high friction torque.

Particle contamination causing the bearing to jam or raising the bearing drag to a large value greater than clutch capacity.

H. External Failures

Possible wrapping of insulation about the shaft causing frictional load which would result in clutch slippage.

I. Multiple Failures

Clutch lock to prevent detenting, followed by failure of shaft bearings with increasing torque load until the gearhead wears out or gears suddenly fail.

Gradual failure of the gearhead by inertia loading during motor reversals.

Sudden failure of the gearhead by gear breakage or jamming during motor reversals.

Evaluation of Possible Failure Modes

Amplifier and Motor Electrical Failures

The Solar Array Drive amplifier was examined to determine the possible failure modes and the effects on the drive motor and telemetry signals due to each failure. The power stage for the solar array drive amplifier is shown in Figure 1 along with the telemetry circuitry. The possible modes of failure are listed below:

a. A short circuit in the output transistor in the motor windings or wiring to the motor.

b. An open circuit in the output transistor, the motor windings, or in the wiring to the motor.

c. Reduction of gain in the output transistors.

In evaluating the failure modes, it is important to know the motor electrical characteristics. These are given in Table I.

TABLE I -- MOTOR ELECTRICAL CHARACTERISTICS

	Phase I	Phase II
Voltage AC RMS	26	18
Frequency (cps)	400	400
Current (amps)	0.064	0.093
Power Input (watts)	1.5	1.5
Power Factor	0.9	0.9
R (ohms)	365	174
X (ohms)	177	85
Z (ohms)	451	216

a. Shorted Transistor or Short on the Motor Winding

If a short occurred in one of the output transistors, 282 milliamperes DC would flow through one-half of the control winding. The power dissipated in the motor winding would be 6.9 watts. Number 40 wire is used in the motor winding and would be unable to carry 282 ma without failing. Also, as can be seen from Figure 1, a short on either side of the motor winding would cause approximately 24 ma DC to flow through the telemetry transformer. Data presented in Table II shows the effect of DC in the primary of the transformer.

TABLE II -- TELEMETRY SIGNAL TRANSFORMER SATURATION CHARACTERISTIC

AC Input Volts RMS	DC Current in Primary Ma	Telemetry Output Volts DC
11.0	0	-3.58
11.0	1	-3.57
11.0	4	-3.53
11.0	7	-3.44
11.0	10	-3.15
11.0	13	-2.76
11.0	16	-2.16
11.0	20	-1.46
11.0	30	-0.64
11.0	32	-0.51

It can be seen from the data that 24 ma DC would saturate the transformer and reduce the telemetry voltage to less than 40 percent of its original value. Since full telemetry voltage was received from the flight vehicle at various intervals during all orbits, a short on the winding or in the output transistor could not have been the reason for the drive failure.

b. Open Transistor or Motor Winding

The telemetry transformer is connected to the supply voltage through the motor winding. If one of the motor windings is open, the telemetry transformer has no return and therefore does not produce the proper transfer function. Data as taken on the solar array drive with one winding open is shown in Table III.

TABLE III -- SOLAR ARRAY DRIVE OPEN WINDING CHARACTERISTICS

Input to SADA Volts DC	Output of SADA Volts RMS	T/M Volts DC	Load in-oz	Speed deg/min	Conditions
0.026	2.45	-0.6	150	3.43	Normal Connections
0.053	1.78	-0.37	150	3.15	One Winding Open
0.031	2.81	-0.72	300	2.94	Normal Connections
0.060	2.10	-0.478	300	3.05	One Winding Open

Maximum voltage with one winding open -- 11.5 VRMS

Maximum telemetry voltage with one winding open -- -2.4 VDC

It can be seen from the data that with one motor winding open, sufficient torque can be supplied to drive the motor at orbital rate. Twice the input voltage is required to do this but the paddles would still track the sun. The drop off in telemetry voltage is evident. With the amplifier saturated the maximum telemetry signal is -2.4 VDC. A 6.4 volt telemetry signal was recorded on those orbits where the paddles were not rotating.

If an output transistor opens, the output voltage to the motor would be the same as in the case of an open winding, but the measured voltage and the telemetry voltage would be higher. The voltage measured across the motor winding is higher because the winding which is not driven acts as an auto transformer and couples approximately 50 percent of the voltage on the driven winding into the open winding. The telemetry transformer has a closed path between the supply voltage and ground and since the peak detector has a long time constant (12 ms), the telemetry transfer function will be nearly the same as it is in the operating conditions.

Data taken with an open transistor are shown in Table IV.

TABLE IV -- OPEN TRANSISTOR CHARACTERISTICS

Output of SADA Volts RMS	T/M Volts DC	Load in.-oz.	Speed deg/min	Conditions
2.45	0.6	150	3.43	Normal
2.56	0.65	150	3.00	Open Transistor
2.81	0.72	300	2.94	Normal
3.09	0.83	300	3.07	Open Transistor

Maximum Output Voltage with Open Transistor -- 18 VRMS

Maximum Telemetry Voltage with Open Transistor -- -5.8 VDC

As can be seen from the data, an open transistor failure might escape detection. The paddles would track, but with twice the normal tracking error. The telemetry voltage drop to -5.8 VDC maximum, however, was not observed and therefore it is concluded this type of failure did not occur.

c. Degradation of Transistor Gain

The solar array drive amplifier is similar in design to the flywheel amplifier which delivers eight times the power of the solar array drive amplifier. The minimum current gain of the output transistors for use as a solar array drive amplifier is 50. This requires each transistor to have a gain of seven. The worst-case gain of the 2N657 is estimated as 20. There is adequate margin in the design to allow one transistor to degrade to a gain of three and still operate normally.

It was concluded that the cause of the solar array drive failure was not a circuit failure. No circuit failure could produce the full range of telemetry signals received from the vehicle.

Clutch and Outer Drive Areas

A key point in the investigation was whether or not the clutch had detented during the lifetime of the spacecraft in orbit and especially during the last hundred orbits when the drive voltage required to maintain orbital rate started to rise from the nominal value of 0.7 volts (TM). If it could be shown that the clutch had not detented, then the drive failure could be localized to those parts of the drive, mechanical and electrical, that precede the output side of the clutch mechanism.

This reasoning would hold true only if it could be demonstrated that the possible failure of the clutch mechanism itself is extremely remote. Therefore, in examining the detent problem, it is necessary to examine closely the possible clutch failure modes to decide if any particular failure is likely to occur in orbit.

The clutch assembly is a ball-detent type device (see Figure 9). The driving member contains a face-plate and a ball cage with eight ball bearings equally spaced circumferentially and bearing axially against the face plate. The driven member contains a face plate with eight conical pockets corresponding to the location of the eight balls in the driving member and is loaded against the driving member by four belleville washers. Normally, the balls are retained in the conical pockets of the driven member and the driver and driven members rotate together without slippage. Under high torque conditions (corresponding to approximately 350 in-oz at the output shaft) the balls are forced out of the ball pockets and a detenting action occurs.

Under clutching action, torque loads are transmitted by a component of ball force against the driven member plate. As torque load is increased, the balls are forced up the incline, moving the plate axially against the spring load. The clutch detents when the balls reach the top surface of the driven plate and the transmitted torque drops to a lower value, approximately one-third of the normal value. The clutch will remain detented until the driver or driven plates are rotated sufficiently to bring the next detents beneath the balls. Detenting action of the clutch is

noticeable on the output trace of the cosine pot by the motion reversal as the balls enter the detents. Recordings made during a test are shown in Figure 10. Under maximum drive voltage, it requires about 47 seconds to drive the balls between centers of adjacent detents when the driven plate is held immovable. The time spent on the flat is 38 seconds and the time on the detent cones is nine seconds. Tests were run on the clutch to measure transmitted torque characteristics at various relative speeds between input and output. The torque waveforms are similar in shape and magnitude.

The flight telemetry records were examined for possible clutch detent operation. If the torque output of the clutch was absorbed by bearing drag, then the varying speed of the motor gearhead should have little or no effect on the output speed of the shaft for a continuously detenting operation of the clutch. As measured from data on various orbits, however, the slewing speed is significantly higher than the orbit speed. When the motor is driven at saturation voltage, the output speed of the shaft does increase, as shown in Figure 11. Figure 11 is the speed-voltage relationship at the motor of the Solar Array Drive with orbital data superimposed. Note that higher voltage produces higher speed throughout the flight to failure. This would not be the case if the clutch had detented.

The speed-voltage relationship at various voltages throughout the mission is of interest in establishing the failure signature. Three points of speed-voltage-torque are available for each orbit:

1. The zero speed voltage -- This is the minimum voltage attained by the amplifier during the dakr period null and corresponds to the minimum frictional torque.

2. The orbit speed voltage -- This is the average driving voltage. The array is tracking the sun and therefore moving at the known orbital rate. The tracking voltage is a measure of the torque load seen by the motor.

3. Slewing speed voltage -- The voltage is known saturation voltage and the slewing speed is measured from the cosine pot data. The array slews approximately 90 degrees in the umbra at a constant voltage input.

The data for a number of representative orbits are shown in Figure 11. Note that the lines shown connecting the data points for each orbit are not lines of constant torque but rather represent the operating line as the drive saw varying torque load with speed changes. From Figure 11, it is evident that the load seen by the Solar Array Drive motor increased steadily. This appears to be indicative of increased friction due to gradual wear, binding, loss of lubrication or from contamination.

Since the analysis of the telemetry data indicated that a clutch detent had not occurred, studies were performed to determine if this lack of detent operation could be due to a failure of the clutch resulting in lock-up in the engaged position. Failures of this type could be obtained in the following manner.

A. Wedging of the detent plate sleeve on the shaft caused by large clearances between the sleeve and shaft.

B. Wedging of the sleeve to shaft under conditions of marginal lubrication and high vacuum.

C. Loss of lubricant causing high frictional forces on bearing surfaces.

D. Wedging of foreign matter between teeth of the input and output clutch pinions preventing relative rotation between the two.

E. Wedging of foreign matter between the belleville washers greatly increasing the apparent spring constant.

F. Deformation of the detent cones into a cup-shaped cross-section due to repeated hammering by drive reversals.

Failure A was investigated and discarded since the maximum tolerance on the clearance of the shaft to bushing is .0008" with a bushing length of .3800 inches. The ratio of clearance to length is such that cocking is highly improbable. In addition, the torque is transmitted across the gear teeth, resulting in a torque about the shaft which would rotate the sleeve and prevent this type of wedging.

Failure B was investigated metallurgically. The shaft is of nitralloy steel and the bushing is of phosphor bronze. Welding of chemically clean surfaces of this type is very unlikely even under large surface pressures. Therefore, this type of failure was considered very unlikely.

Failure C was investigated experimentally. A lubricated clutch assembly was detented through each position of the balls in both directions. The torque at each position was recorded. The clutch was chemically cleaned to remove all lubricant, and re-assembled. The test was rerun. Torque levels at detent were similar. Therefore, simple lubricant loss was not considered to cause a failure.

Failure D would tend to be cleared out, if it had occurred, by the application of reverse drive torques which did occur a number of times on each orbit. This cause was considered to be remote.

Failure E does not appear to be possible as it would take a significant force to insert any large particles between two facing washers and could not occur in the assembled drive.

Failure F was evaluted experimentally by applying 2000 reversing cycles at fifteen-second intervals to the solar array drive with the output side of the clutch pinned. No measurable difference between detent torques before and after the test was obtained. Therefore, this type of failure was considered to be unlikely.

It was concluded that the clutch did not fail in the locked condition.

Therefore, since it was concluded that the clutch operation was normal and had neither detented nor locked-up, all hypothesized failure modes on the outboard side of the clutch could not have occurred during the flight of Nimbus I. The failure must have been, therefore, in the motor or the gearhead of the Solar Array Drive.

Motor Temperature Evaluation

Thermal tests were made with a drive motor to determine the extremes of temperature that might have been experienced during ground testing and operation in orbit. Although the motor itself was built to take a 200°C temperature without failure, it was realized that the lubricant life could be seriously shortened by high temperature, especially when worked in a high speed bearing. This would result in shortening bearing life.

Temperature tests under vacuum conditions were run on a motor operating normally and with a locked rotor. Since the maximum power is absorbed in the motor under stalled conditions with a locked rotor, it was expected that the maximum temperatures should be reached in the rotor under these conditions.

The motor under test was mounted to a servo-breadboard plate (see Figure 12) with the rotor locked by means of a meshing gear which was fixed to the plate but thermally isolated from the plate. Thermocouples were attached to the rear bearing outer race, inner race and shaft; to the front motor shaft, mounting plate, and gear; and to the motor housing. The motor was first tested without the cover or Nylasint reservoir in the air, and then in vacuum. Next the cover and reservoir were installed and temperatures again checked. Finally, the motor was attached to the gearhead with the reservoir and cover attached and temperatures recorded in vacuum for the no-load conditions. Temperatures of the rotating rotor and shaft could not be monitored for this test.

The power supplied to both the reference and control windings was varied during each test to obtain the equilibrium temperatures for various power inputs. Analysis of the data indicated that the normal orbital driving voltage condition on themotor would lead to maximum temperatures in the motor of less than 150°F.

Figure 13 shows the temperature rise in vacuum of the hottest measured points on the motor, both stalled and running. Figure 14 shows the thermal response of selected points on the motor for both power-applied and power-removed conditions. The thermal time constant is approximately twelve minutes.

Under slewing rate conditions with maximum power input and the highest control box ambient temperatures, the data indicated that the motor bearing local temperatures would not have exceeded 210°F. Based on the published data for G300 grease, this temperature was not high enough to have caused serious degradation of the lubricant. However, it was realized at this point that the actual operating rotor temperature might be greater than that indicated by the tests and that the G300 grease might have lower temperature limitations than data to date indicated, and therefore lubricant deterioration was still a distinct possibility.

Pre-Flight Test History

The pre-flight test history of the Solar Array Drive was reviewed. The operating time and environments are shown in Table II. No significant test events were discovered in reviewing the data which appeared to be related to the flight failure.

TABLE II -- SOLAR ARRAY DRIVE TEST HISTORY
(all data in hours)

TEST	ORBIT RATE	SLEW RATE	POWER ON
Ambient	307	45	2010
Vac-Thermal	27	156	1320
Total	334	201	3330
ORBIT	440	44	625

No data is available on the number of reversals experienced in test. Paddle inertias were not simulated. Approximately 2300 reversals occurred in orbit including those reversals that occurred due to pitch oscillations of the vehicle.

Analysis of Design Implementation and Quality Control

In order to investigate the degree of probability that the flight failure might have been due to implementation or quality control defects, several motor-gearhead units and one complete Solar Array Drive were completely disassembled and inspected. The lubricant quantity and quality were evaluated; clearances, finishes and hardnesses were determined. Disassembly was performed in a Clean Room and the location and quantity of built-in contaminant was assessed. Parts were checked for adherence to drawings, assembly and good-practice procedures.

A number of design implementation and quality control deficiencies were found but there were none that indicated the cause of the flight failure. All of the units had had some test operations performed; some evidences of wear were found.

Among the design deficiencies found were (1) an extremely small air gap between the motor rotor and stator (.0005 in), (2) use of crown retainers instead of ribbon retainers in the ball bearings, (3) a direct venting path from the back of the motor to the vacuum environment which exposed the lubricant to hard vacuum, (4) poor material and heat treatment selection for the gearhead gears, and (5) two-piece, pressed-on gear and shaft construction.

Among the quality control deficiencies were (1) several kinds of contamination (chips, dirt, insulation), (2) improper soldering techniques, (3) improper heat treatment, (4) insufficient lubricant, (5) improper assembly (loose screws, loose fits between bearings and shafts and housings), (6) poor wire dress, and (7) improper machining.

None of these defects would have caused the flight failure nor would necessarily have produced other failures, though each degraded the margin between successful operation and malfunction of the unit.

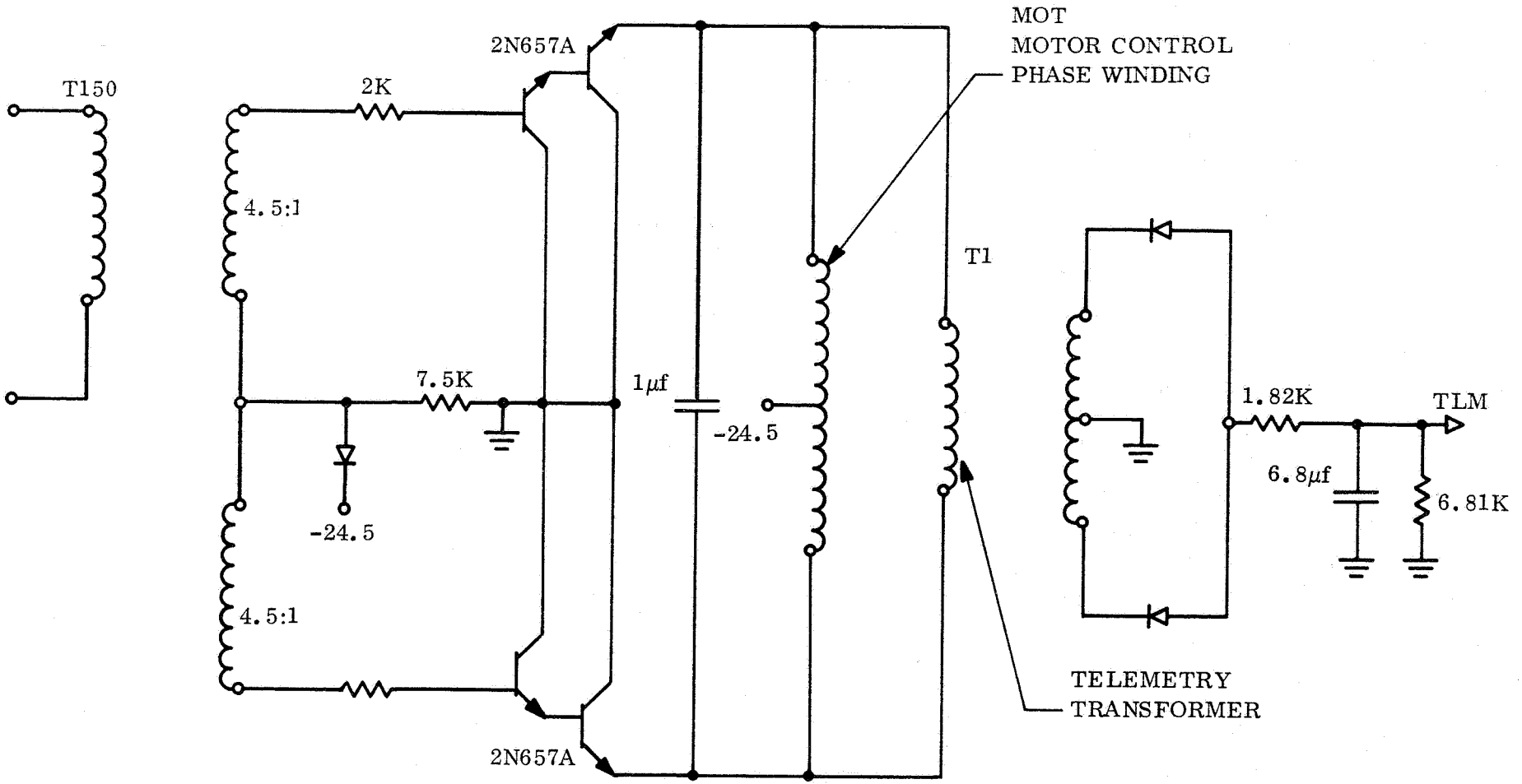

Section 3, Figure 1
Solar Array Drive Amplifier Output Circuitry

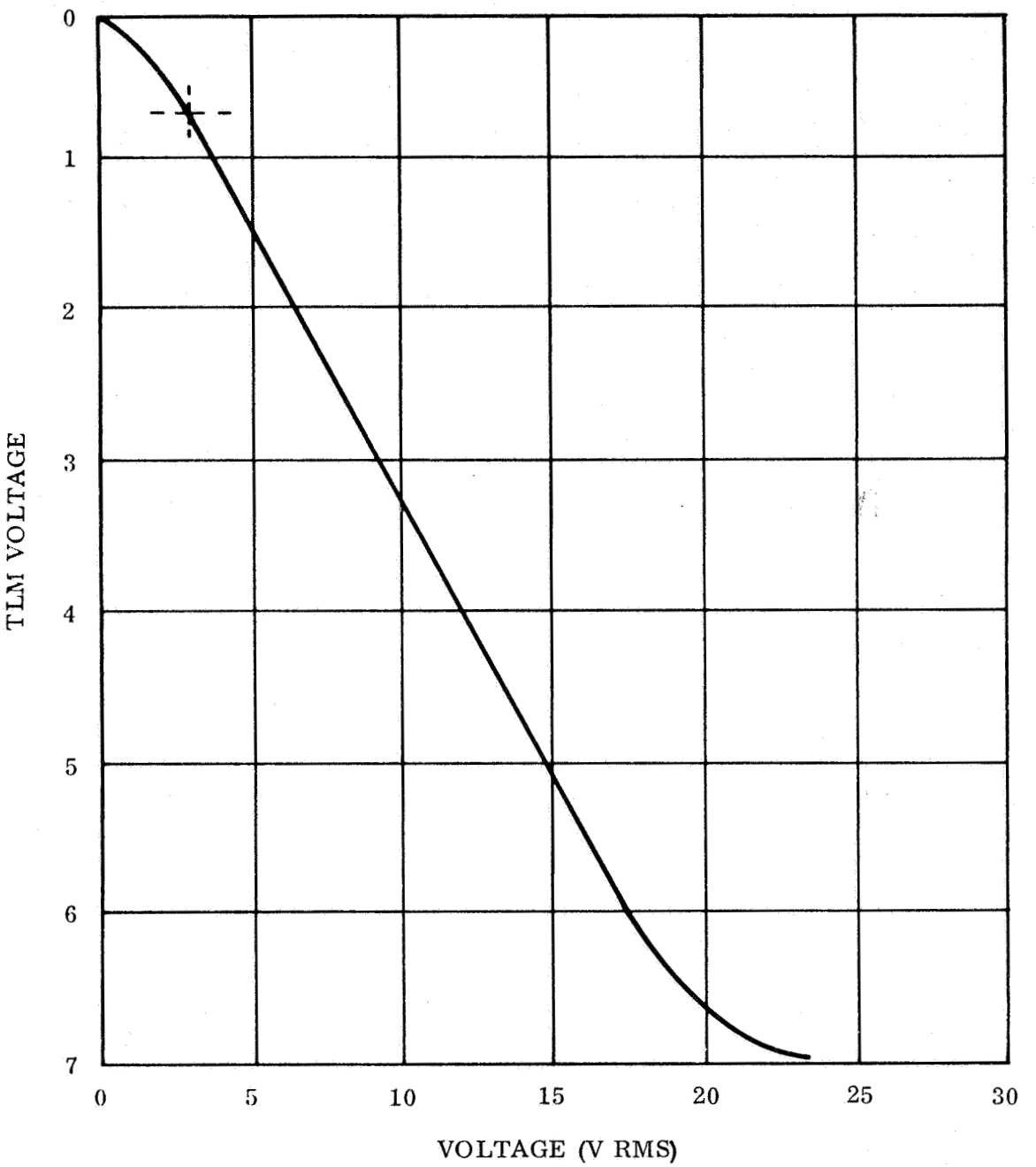

Section 3, Figure 2
Solar Array Drive Amplifier Output vs. TLM Voltage

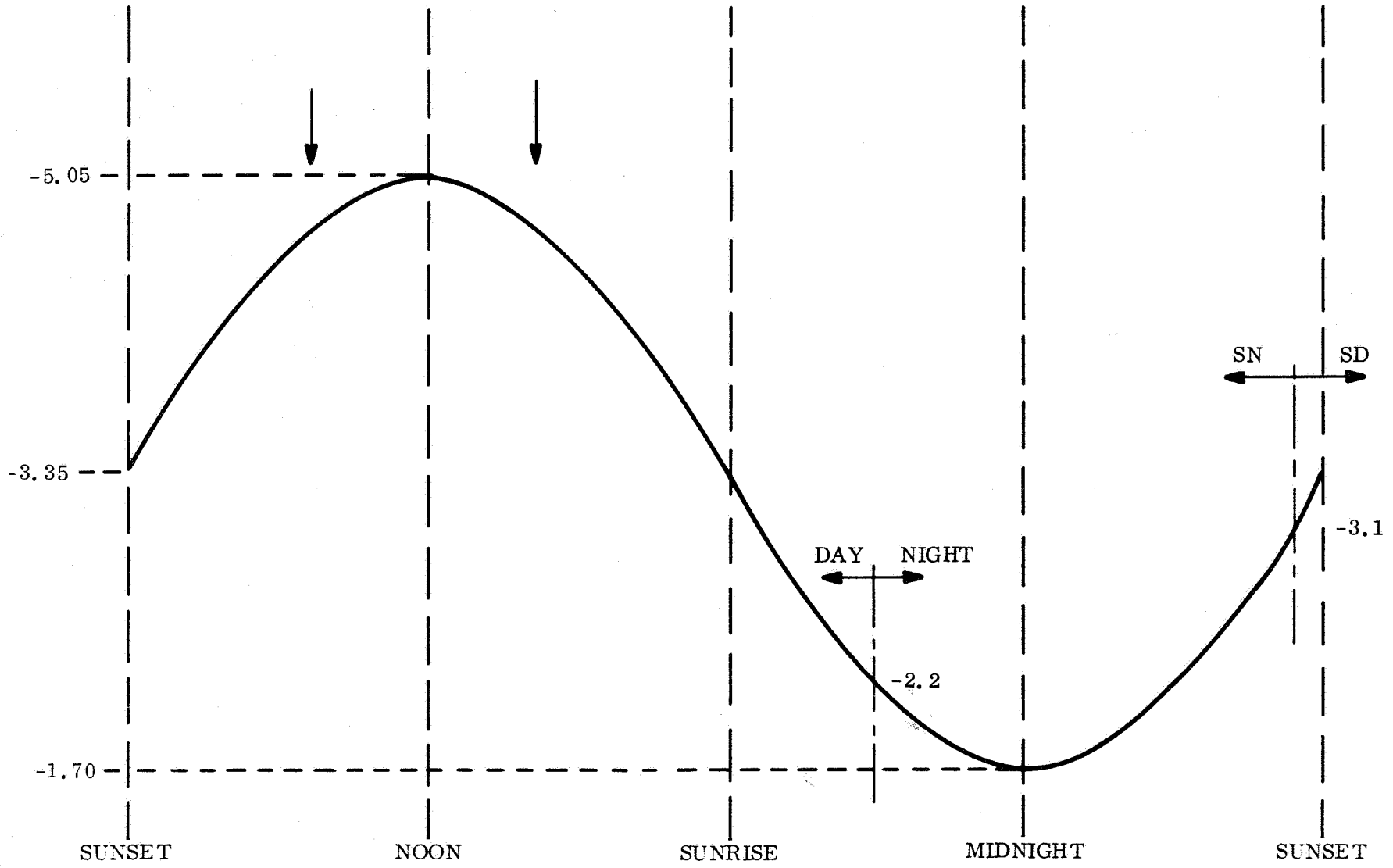

Section 3, Figure 3
Cosine Pot Telemetry Voltage vs. Shaft Position

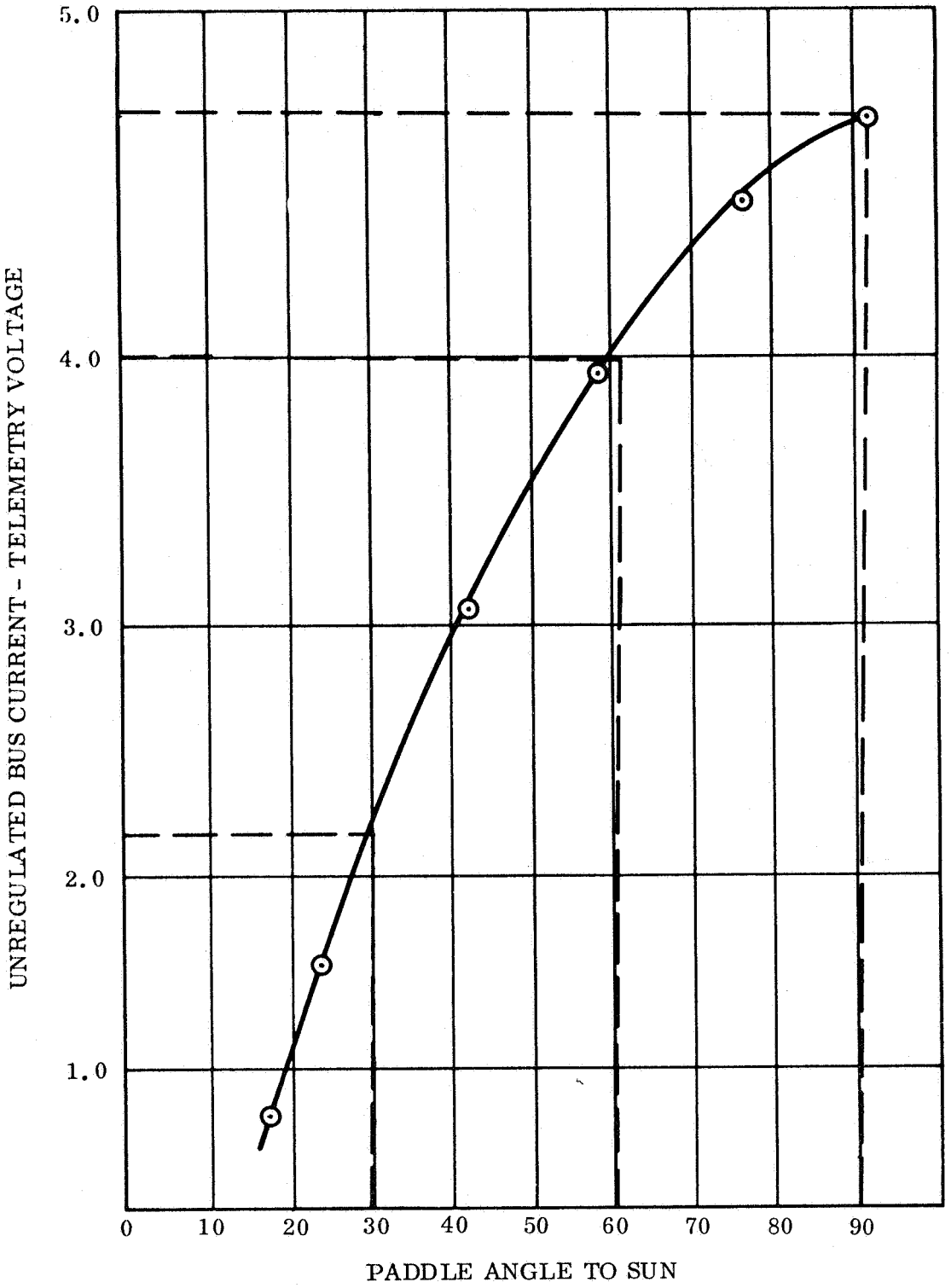

Section 3, Figure 4
Unregulated Bus Current vs. Paddle Angle

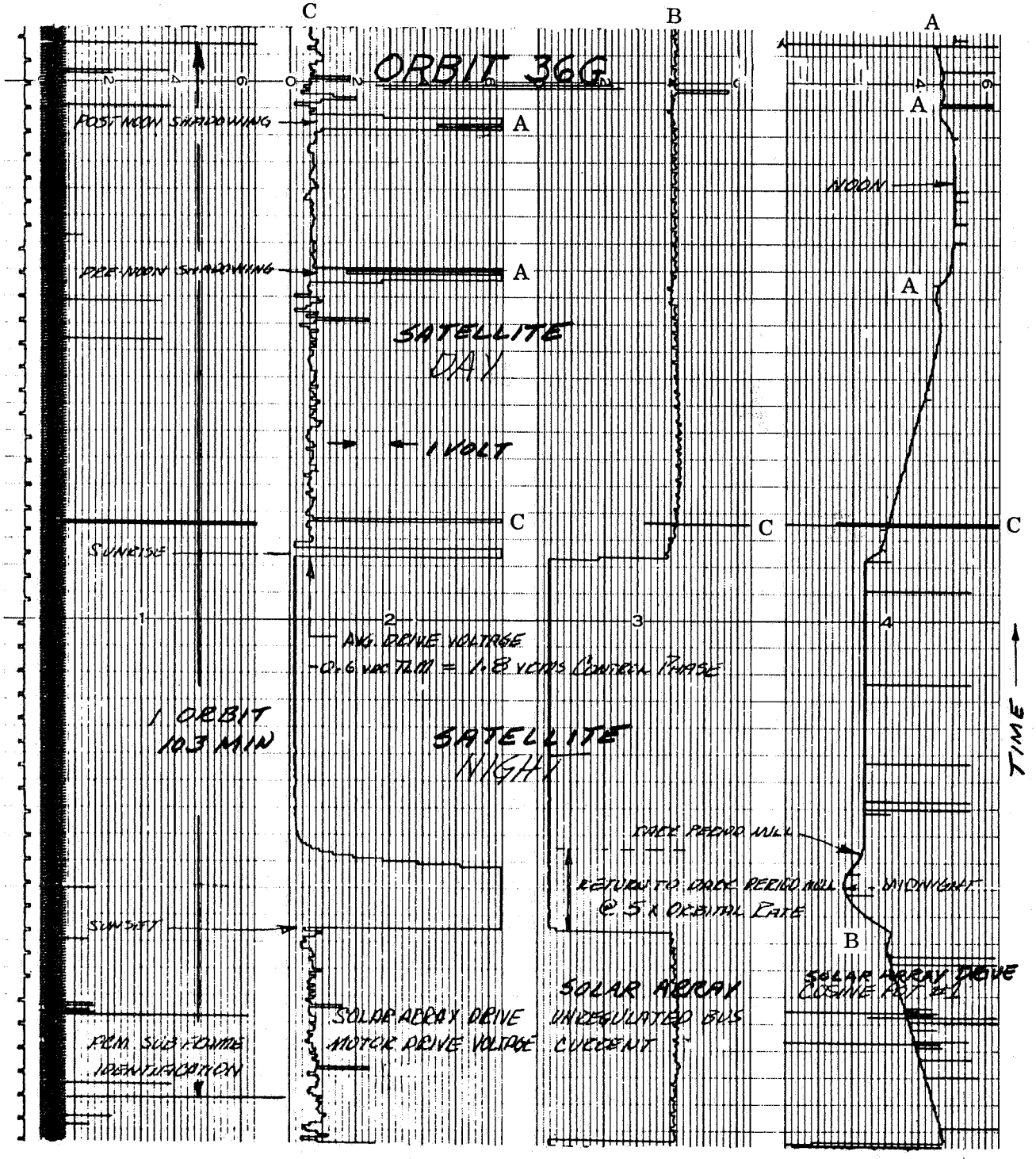

Section 3, Figure 5
Solar Array System TLM, Orbit 36

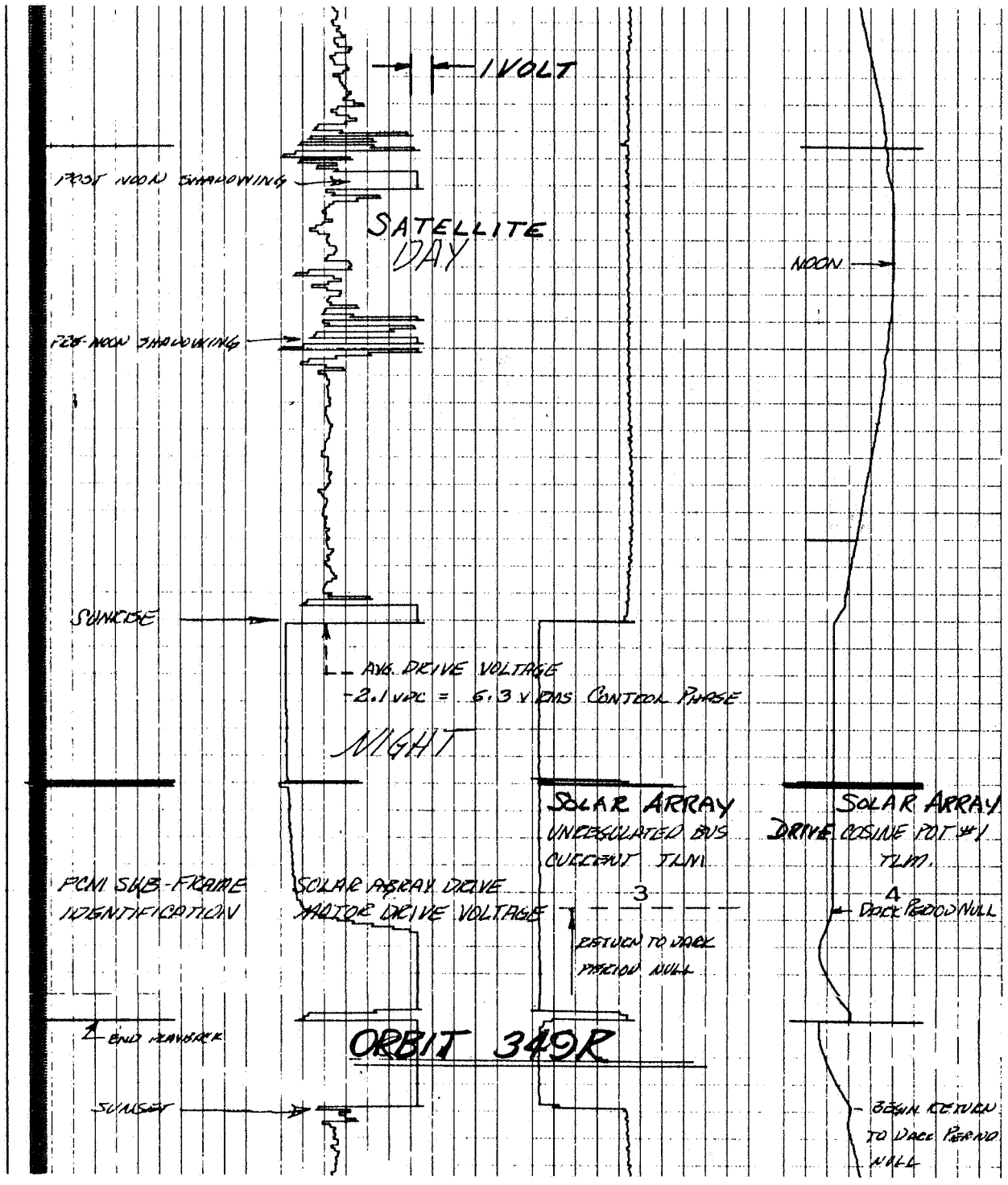

Section 3, Figure 6
Solar Array System TLM, Orbit 349

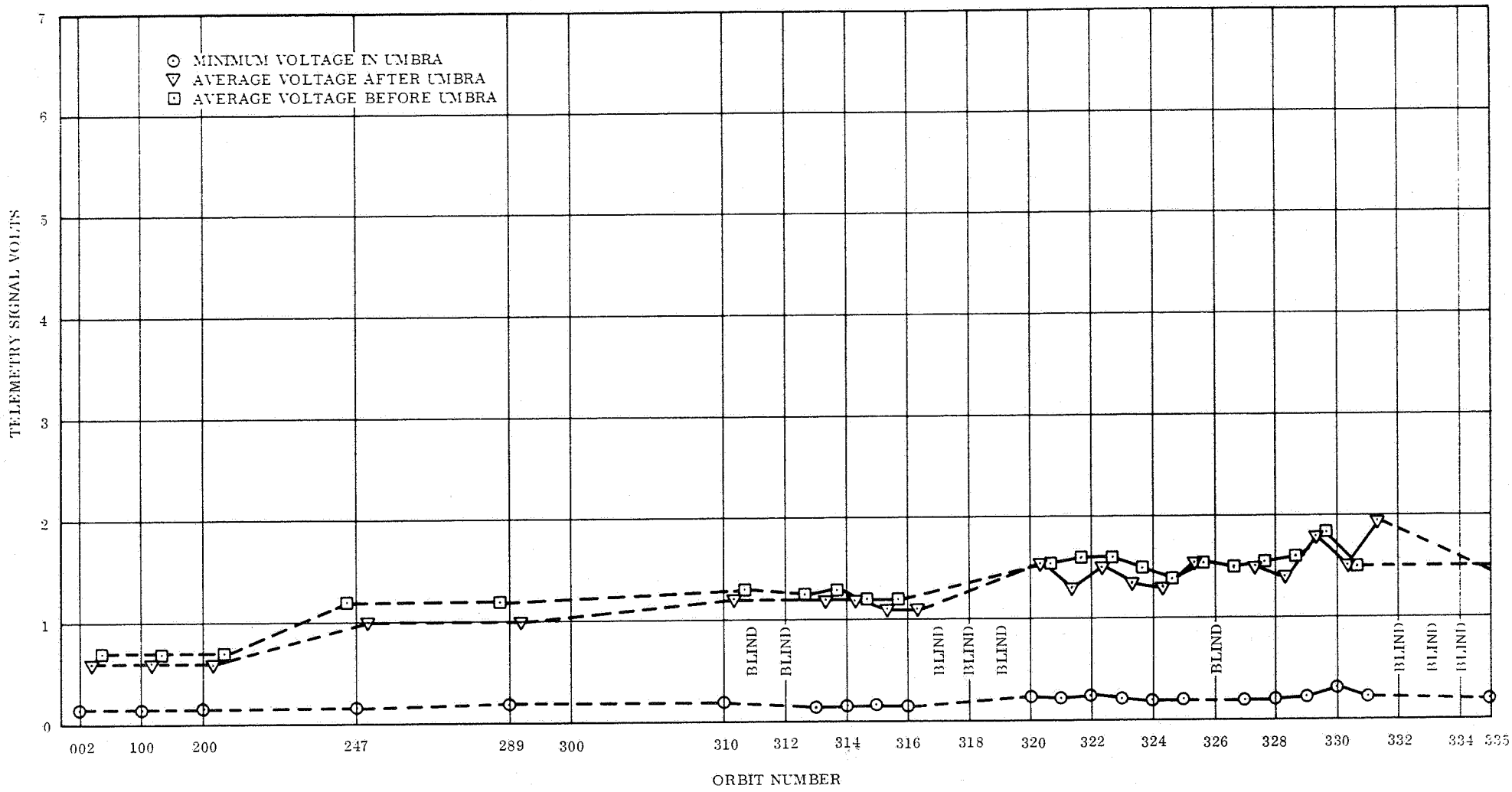

Section 3, Figure 7
Solar Array Drive Voltage History (1)

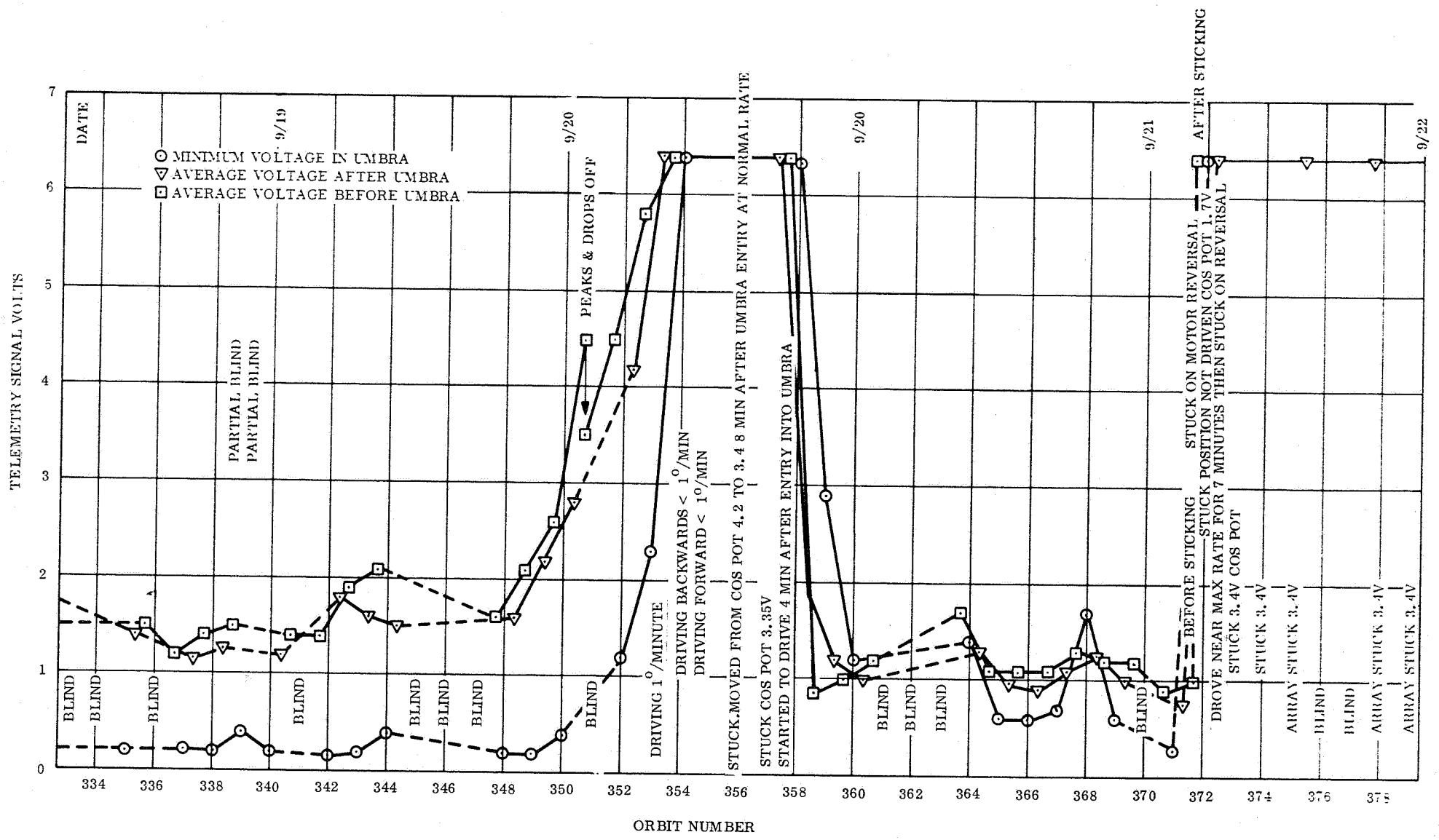

Section 3, Figure 8
Solar Array Drive Voltage History (2)

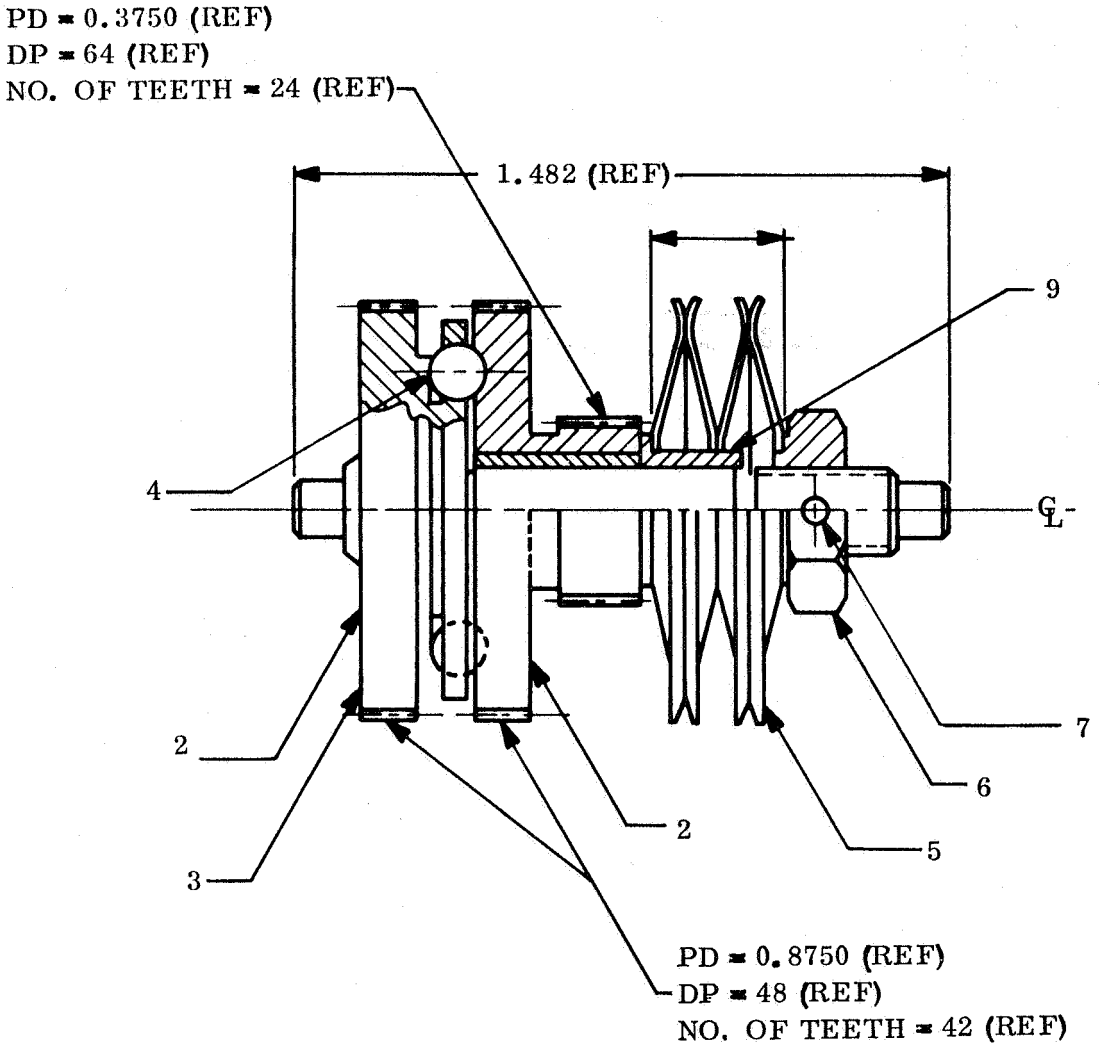

Section 3, Figure 9
Clutch Assembly

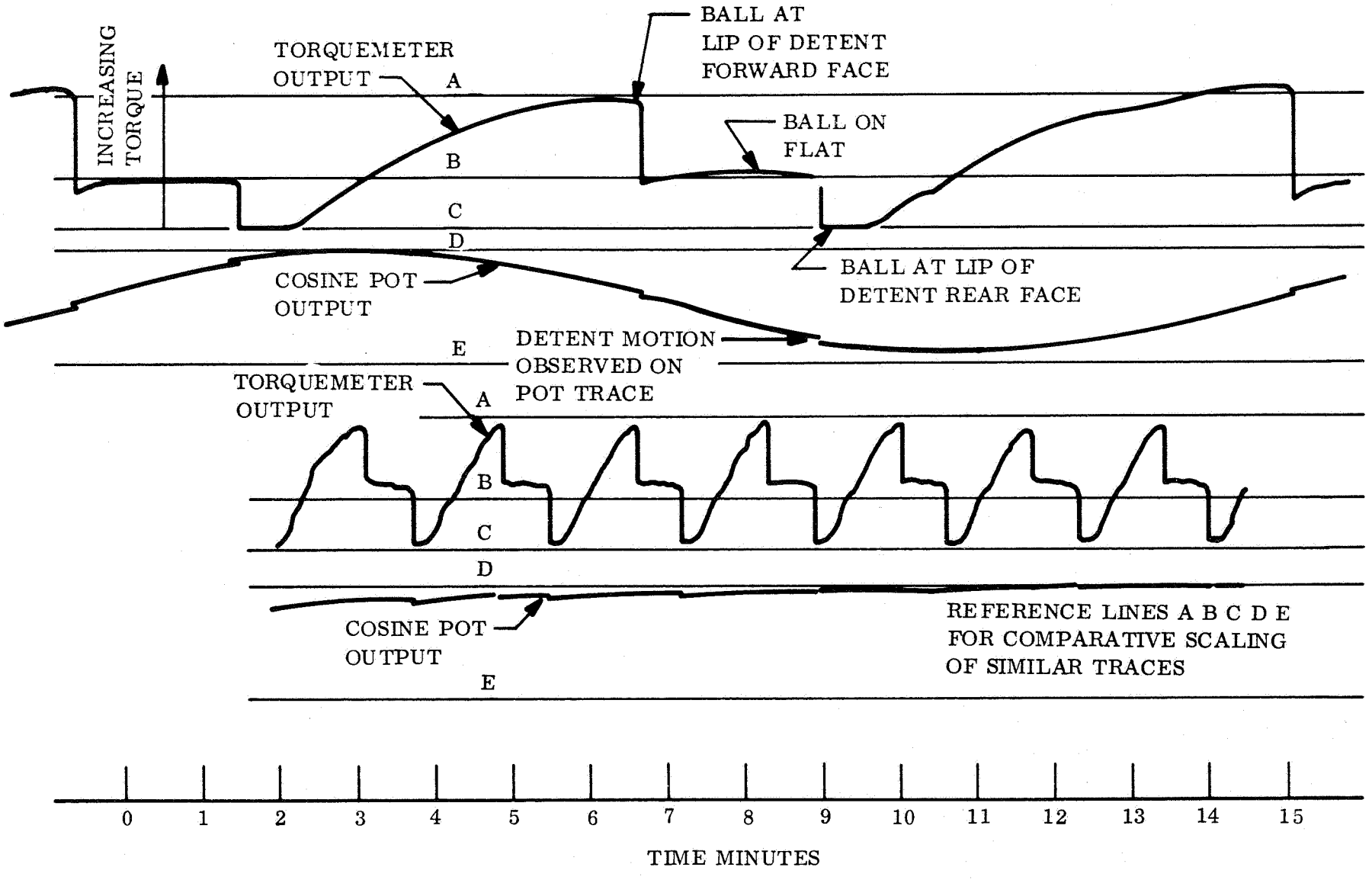

Section 3, Figure 10
Clutch Torque Transmission & Detent Action

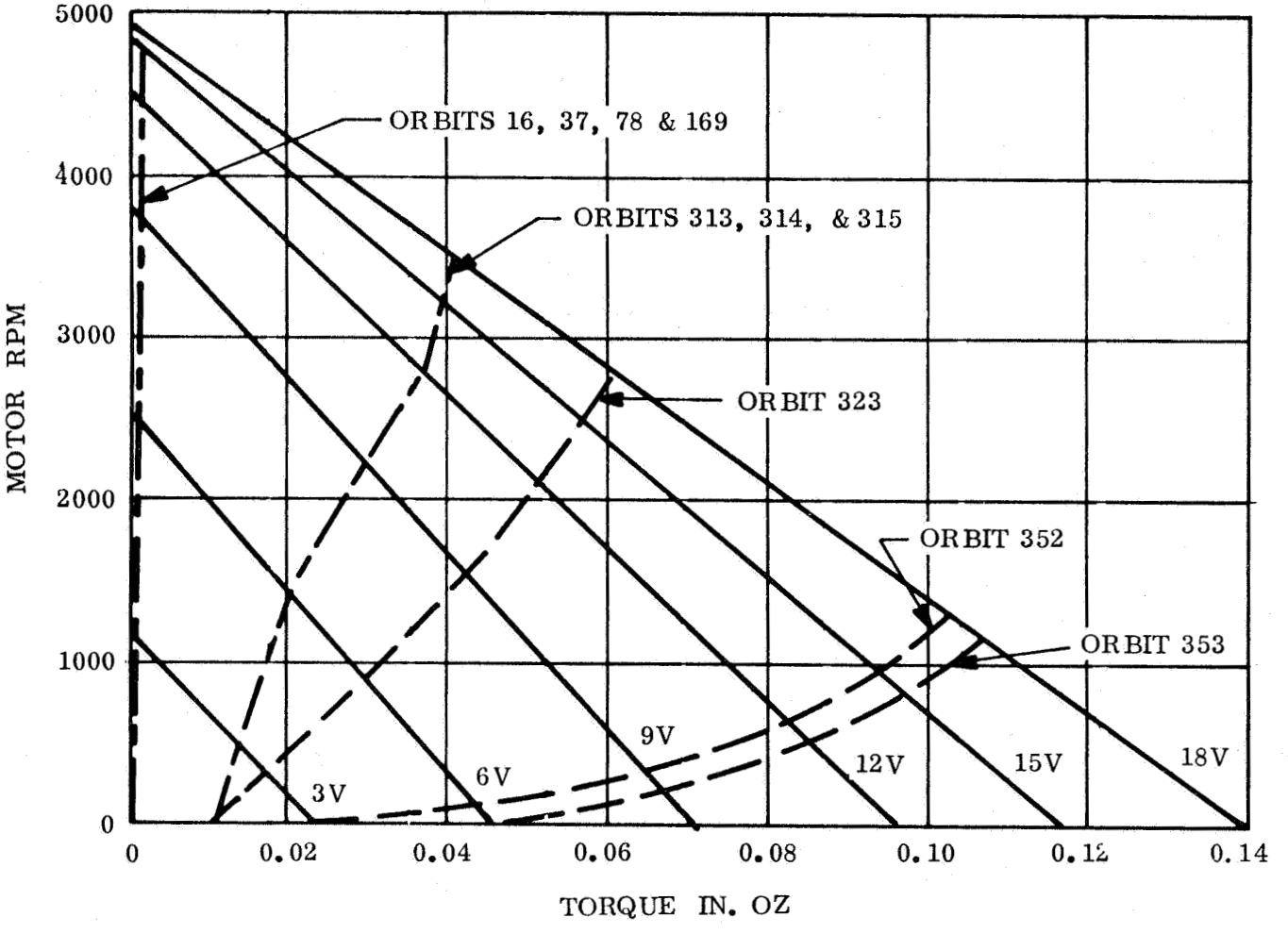

Section 3, Figure 11
Solar Array Drive Motor Speed.
Orbital Data Superimposed

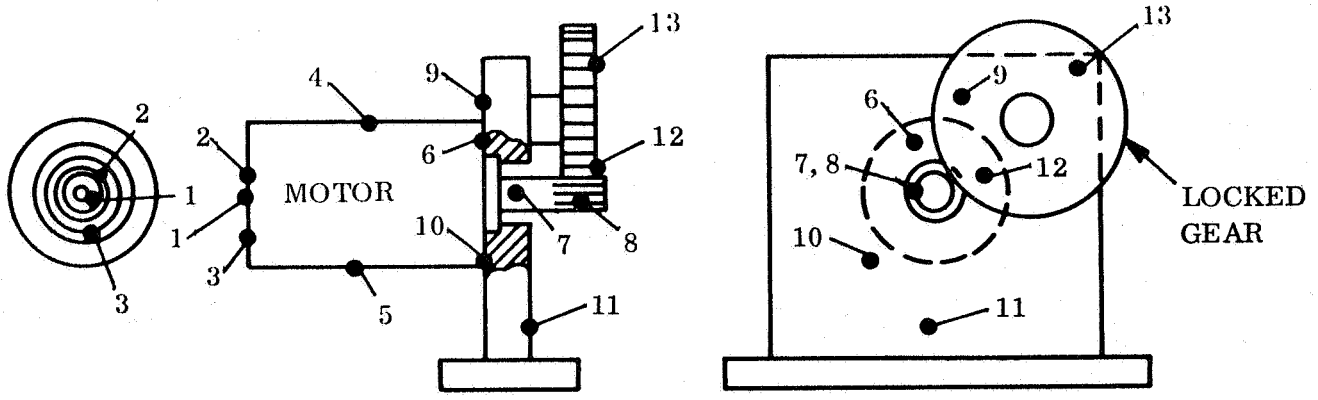

LOCKED MOTOR TEST

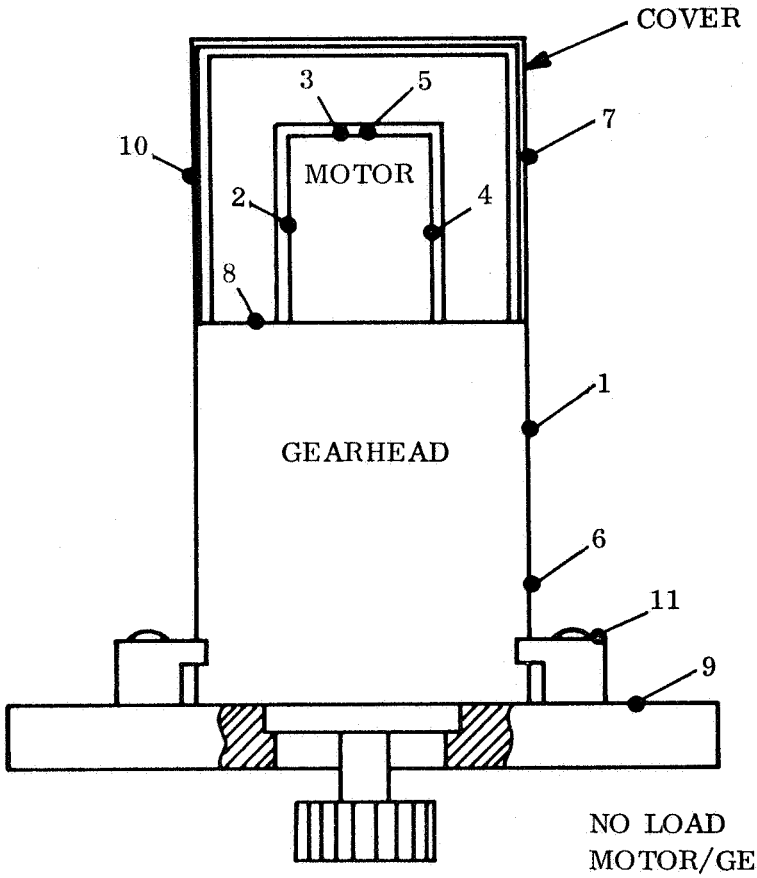

NO LOAD
MOTOR/GEARHEAD
TEST

Section 3, Figure 12
Thermocouple Locations, Temperature
Rise Tests

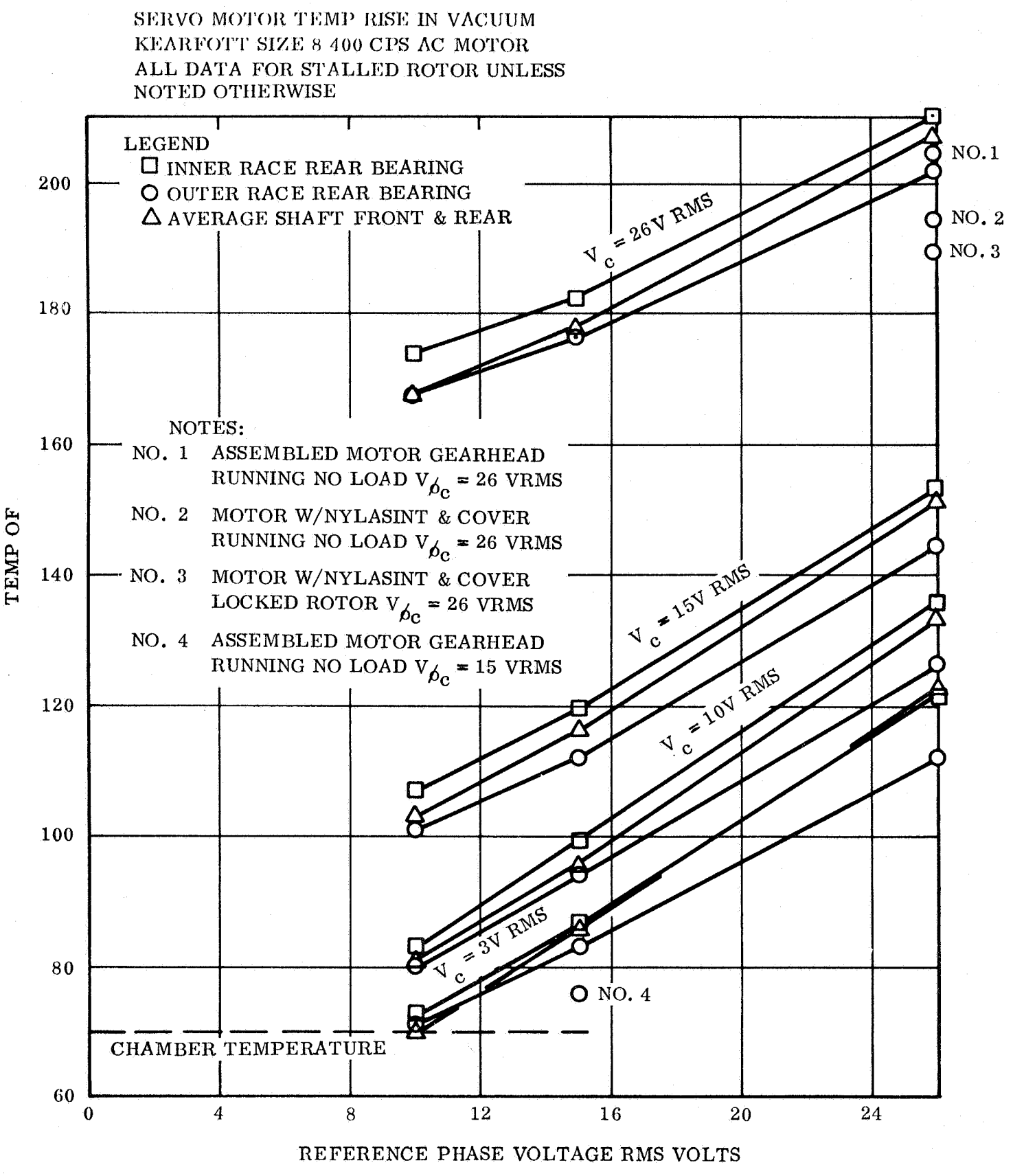

Section 3, Figure 13
Motor Gearhead Temperature Rise in Vacuum

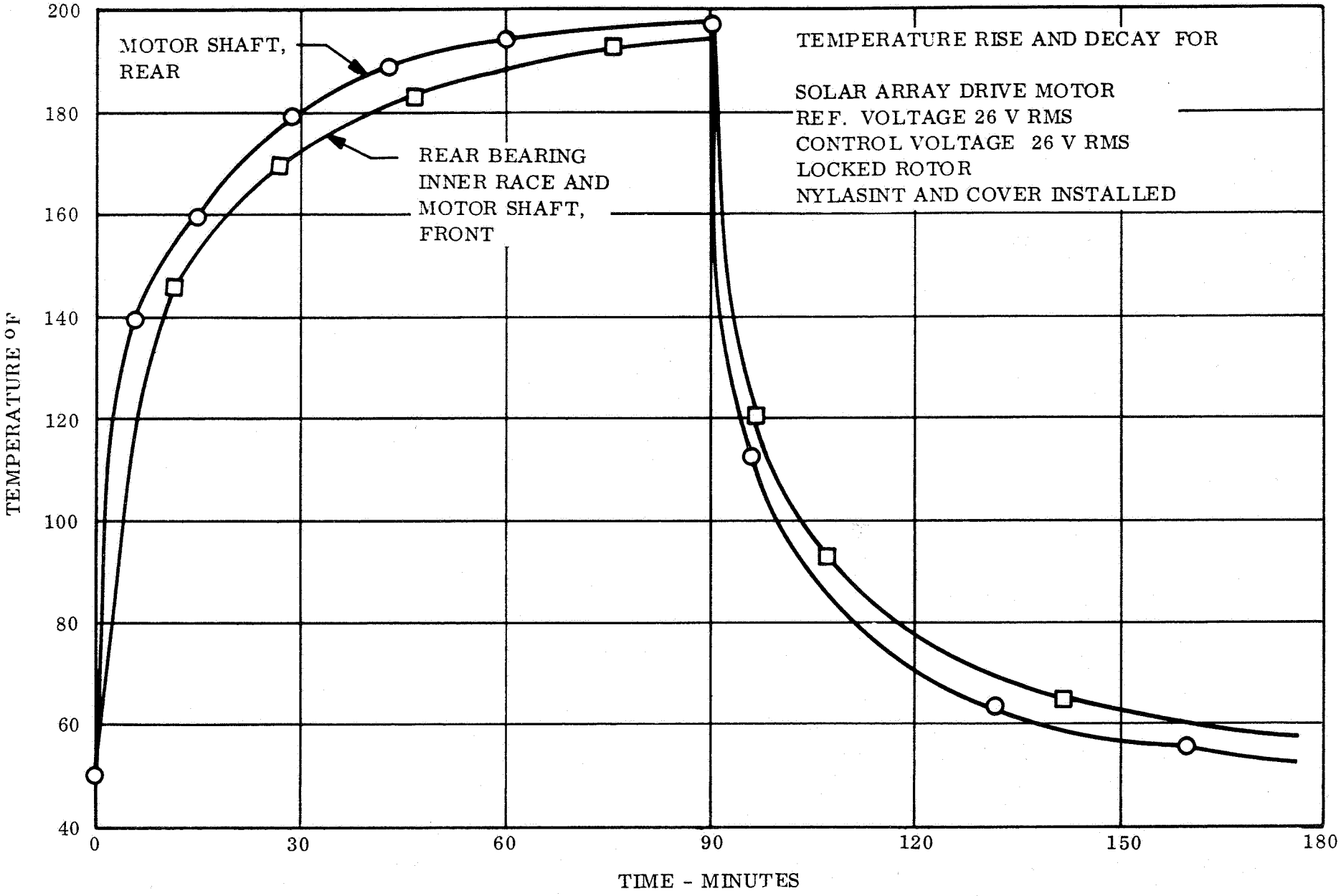

Section 3, Figure 14
Temperature Rise and Decay Time

4.0 FAILURE VERIFICATION PROGRAM

Introduction

Proceeding on the hypothesis that the flight failure was due to a failure in the Solar Array Drive and that the failure could be reproduced in the laboratory, a failure verification program was established. A series of tests were set up using units comparable to the flight hardware. At the same time, investigations were begun to determine the maximum motor bearing and lubricant temperatures and to establish the suitability and limitations of G-300 grease and other high-vacuum lubricants in similar applications. Lastly, a series of reviews with leading experts in the field of lubrication were held to ensure consideration of experience in related applications.

Summary and Conclusions

The failure verification program produced positive evidence of the cause of the flight failure. The flight failure signature was reproduced by laboratory testing. Subsequent teardown showed that the failures were due to motor bearing lubricant degradation. Studies and tests showed that high temperatures existed within the motor at the rotor and bearings. The lubricant investigations and testing had indicated these temperatures would produce lubrication difficulties. It was therefore concluded that the flight failure was due to an inherent design condition whereby when the Solar Array Drive was operated for prolonged periods in vacuum, the motor bearing lubricant degraded due to high temperature.

Failure Verification Testing

The failure verification tests consisted of simulated flight operation, in vacuum for prolonged periods, of units similar or identical to the Nimbus I flight hardware. The units for these tests were used as is, without disassembly or inspection except that some instrumentation sensors were attached. Three motor gearhead units were tested without external load, at maximum speed and voltage and at various environmental temperatures.

One complete Solar Array Drive was tested in a similar fashion. One vehicle with a complete Solar Array Subsystem less the Solar Array Paddles, but with a braking load, was tested in vacuum to an orbital cycle closely corresponding to that of Nimbus I. Another vehicle with a complete Solar Array Subsystem and large inertia wheels to simulate the inertia of the Solar Array Paddles was similarly tested.

All of these tests produced failures. The failure signatures were almost identical to the flight failure. Two motor-gearhead units disassembled, refurbished, and relubricated with newly-produced G-300 grease, but otherwise of the same configuration, also showed clear indications of failure after being tested under simulated flight conditions. Figure 1 presents a summary of the individual tests and the subsequent disassembly analyses.

In every case, the speed of the motor gearhead unit slowed down and became erratic in operation; some units were tested to the point of complete motor stall. In every case but one, upon subsequent teardown and inspection, the failure was found to be due to deteriorated grease (thickened and discolored) in the motor bearings, which caused high bearing torque and slowed or stalled the motor. The single exception was a unit which was found to have degraded grease on the gears in the first pass of the gearhead. Vendor data shows that this unit was significantly different in operation immediately after assembly and it is presumed that some anomaly occured at the vendor's plant which introduced the degraded grease. The two rebuilt units experienced motor speed slowdown and grease deterioration in approximately the same average test time as did the as-is units, which indicated that the shelf life of the grease was not a significant factor in the flight failure.

It should be noted that because the normal output torque of the motor was so low, approximately .12 in.oz., it did not take very much increase in motor bearing drag torque to produce motor stall. Consequently, no parts were found to be badly damaged; even the balls and races of the motor bearings would have been servicable for many more hours if the motor had had a higher torque capability.

Motor Bearing Temperature Investigation

It was suspected that the post-flight analysis temperature tests had yielded results which were considerably lower than those actually experienced within the motor unit at the motor bearings when the unit was operating. Accordingly, it was decided to investigate further, both analytically and by testing. The analytical study utilized a combination of empirical and theoretical relationships to make parametric equations which were then solved with a PACE computer and presented in curve form. These curves indicated that high temperatures existed at the inner race and motor shaft.

Measurement of actual motor bearing temperatures was performed by a novel technique developed for this investigation. The motor was run in a vacuum chamber with its rear bearing exposed and scanned externally through a KBR window by an infrared sensing radiometer (see Figure 2 and Figure 3). The method by which the temperatures were obtained was rather complex because of the difficulty of obtaining a true temperature calibration. It was necessary to set up a dummy bearing having a known, fixed temperature over the entire surface of the bearing and with similar IR radiation characteristics such as the same configuration, materials, and surface treatment. The radiometer was made to scan across this bearing and a recording of radiometer output versus scan position made. This procedure was repeated at various temperature levels to produce a set of calibrating curves. The radiometer then was made to scan the motor bearing while the motor was operating at stabilized conditions and a recording of the radiometer output was made. As an additional calibration check, a thermocouple was attached to the outer race of the bearing and read simultaneously when the radiometer scanned this area. A typical recording of the radiometer scan is shown in Figure 3. The recorded outputs during the dummy bearing and motor bearing scans were then compared and the true motor bearing temperatures determined by interpolation of the data. By this means the actual rotor shaft, ball bearing inner race, ball retainer, and outer race temperatures were measured while the rotating parts were operating normally. These measurements indicated temperatures in excess of 300^{o}F at

the bearing inner race and ball retainer at the same time that the outer race and motor bearing were running much cooler at less than 200°F, which was the maximum temperature measured previously by conventional thermocouple techniques (see Figure 4).

Lubricant Investigation

The investigation into lubricant characteristics and limitations showed that the G-300 silicone grease should be suitable for the application but must be suffering degradation by some means, probably high temperature in excess of 200°F. An extensive search of published literature on high vacuum lubricants and on similar applications to that of the Solar Array Drive was made. These studies indicated that under apparently similar laboratory conditions and actual applications, G-300 grease had performed well for thousands of hours and was equal or superior to any other vacuum lubricant. Similarly, accelerated tests of grease samples in vacuum in Spacecraft Department laboratories showed that the G-300 grease would retain its essential characteristics for extremely long periods in vacuum at temperatures up to 200°F, but that losses accelerated at higher temperatures.

Consultant Reviews

All through the failure investigation program, reviews with the consultant experts in lubrication ensured that the activities undertaken and an analysis of the results obtained were consistent with the latest state-of-the-art knowledge. The following persons participated in the program:

W. E. Campbell, PhD, Rensselaer Polytechnic Institute
J. Cerrini, Naval Air Material Center
F. Clauss, PhD, Lockheed Missile and Space Division
M. Devine, Naval Air Material Center
D. Flom, PhD, GE, Space Sciences Laboratory
A. Haltner, PhD, GE, Space Sciences Laboratory
R. Johnson, NASA, Lewis Research Laboratory

RESULTS OF FAILURE VERIFICATION TESTING

UNIT	TEST DATA	POST-TEST TEARDOWN OBSERVATIONS		
		MOTOR	GEARHEAD	OTHER AREAS
MGH # 5 P 1	Stopped @ 330 hrs.	High bearing Torque. Thick grease.	Operation normal. Dry grease, high speed end.	-----
MGH # 8 P3	Stopped @ 29 hrs.	Normal.	Degraded, thick grease on first pass mesh.	-----
MGH # 4 P1	Stopped @ 200 hrs.	High bearing torque. Thick grease.	Operation normal. Dry grease, high speed end.	-----
S.A.D. # 9 MGH # 1	Stopped @ 160 hrs.	High bearing torque. Thick grease.	Operation normal. Dry grease, high speed end.	Normal Operation & appearance.
Proto Vehicle S.A.D. # 8	Stopped @ 1200 hrs. Restarted. Stop test @ 1400 hrs.	High bearing Torque. Thick grease.	Operation normal. Dry grease, high speed end.	Normal
V-2 Vehicle S.A.D. # 1	Stopped @ ≈ 400 hrs.	High bearing Torque. Thick grease.	Operation normal. Dry grease, high speed end.	Normal
MGH # 8 P1	Slowed down @ ≈ 300 hrs. Stopped test @ ≈ 400 hrs.	Degraded grease areas on bearings.	Operation normal. Appearance normal.	-----
MGH # 8 P3	Slowed down @ ≈ 300 hrs. Stopped test @ ≈ 480 hrs.	Degraded grease areas on bearings.	Operation normal. Appearance normal.	-----

SECTION 4, FIGURE 1

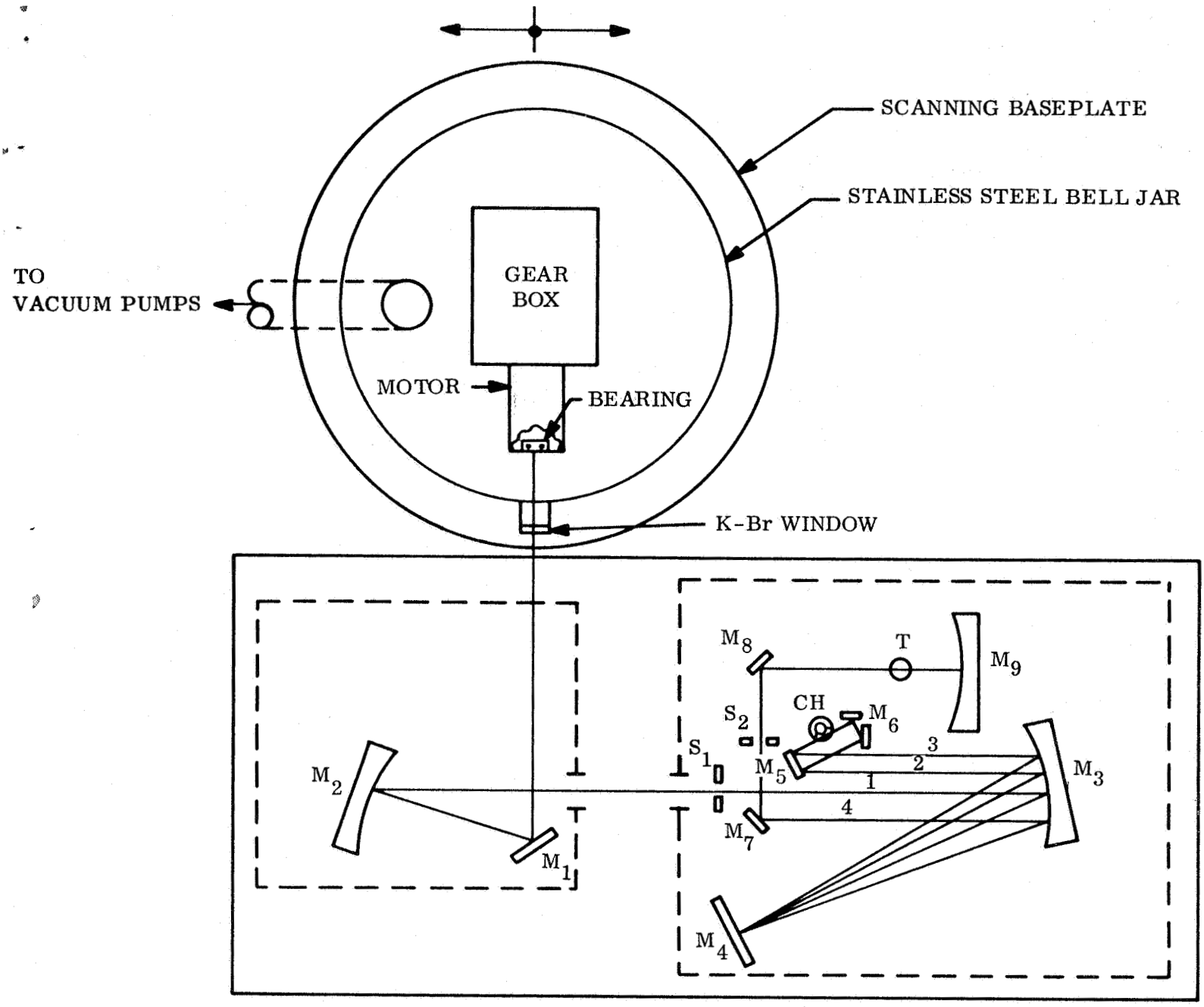

M_1; M_4; M_5; M_6; M_7; M_8 = FLAT FRONT SURFACE MIRRORS
M_2 = SPHERICAL MIRROR
M_3 = PARABOLIC MIRROR
M_9 = ELLIPTICAL MIRROR

Section 4, Figure 2
Sketch of Test Setup for IR-Scanning of a
Rotating Motor Bearing

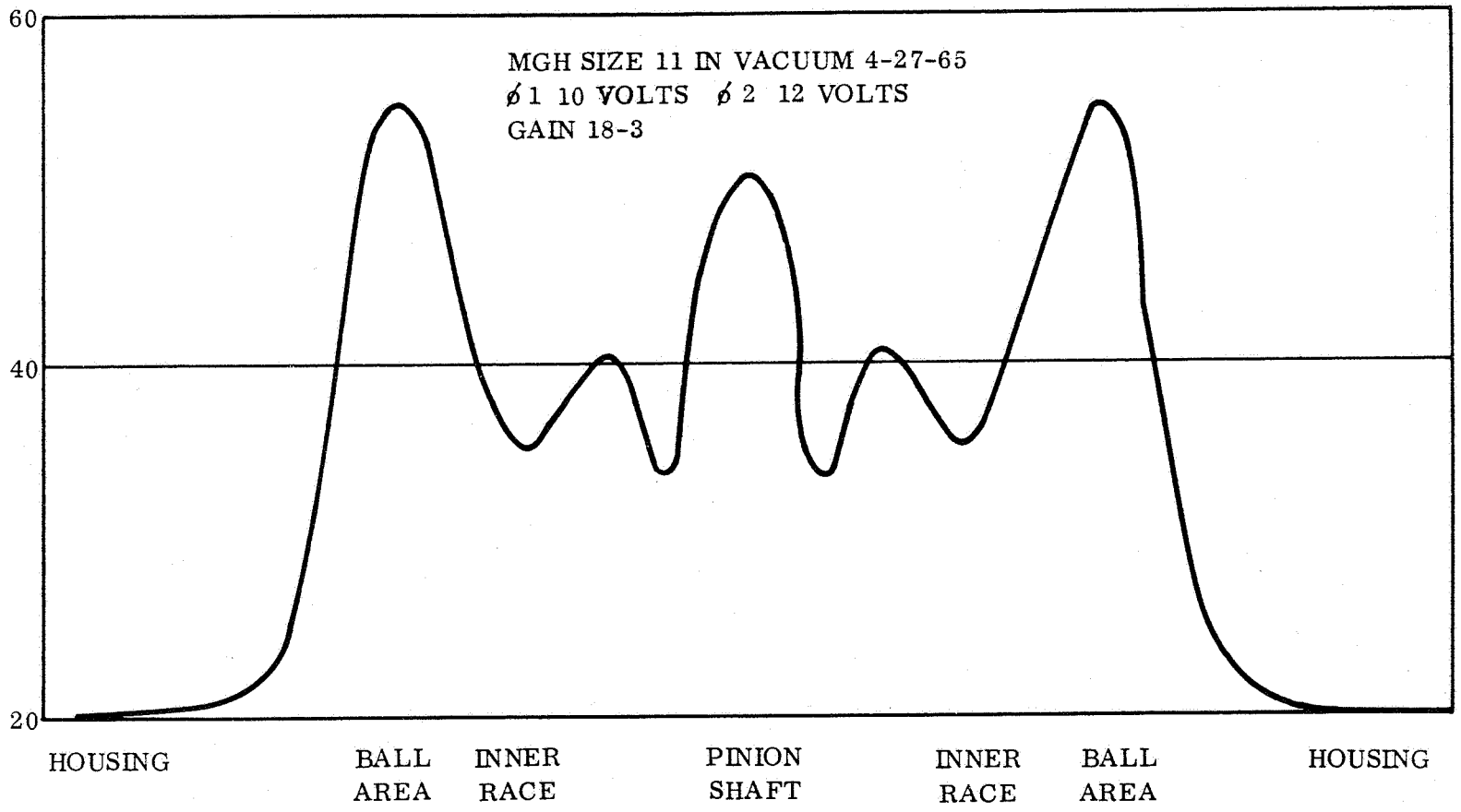

Section 4, Figure 3
Typical Radiation Profile for Operating Motor

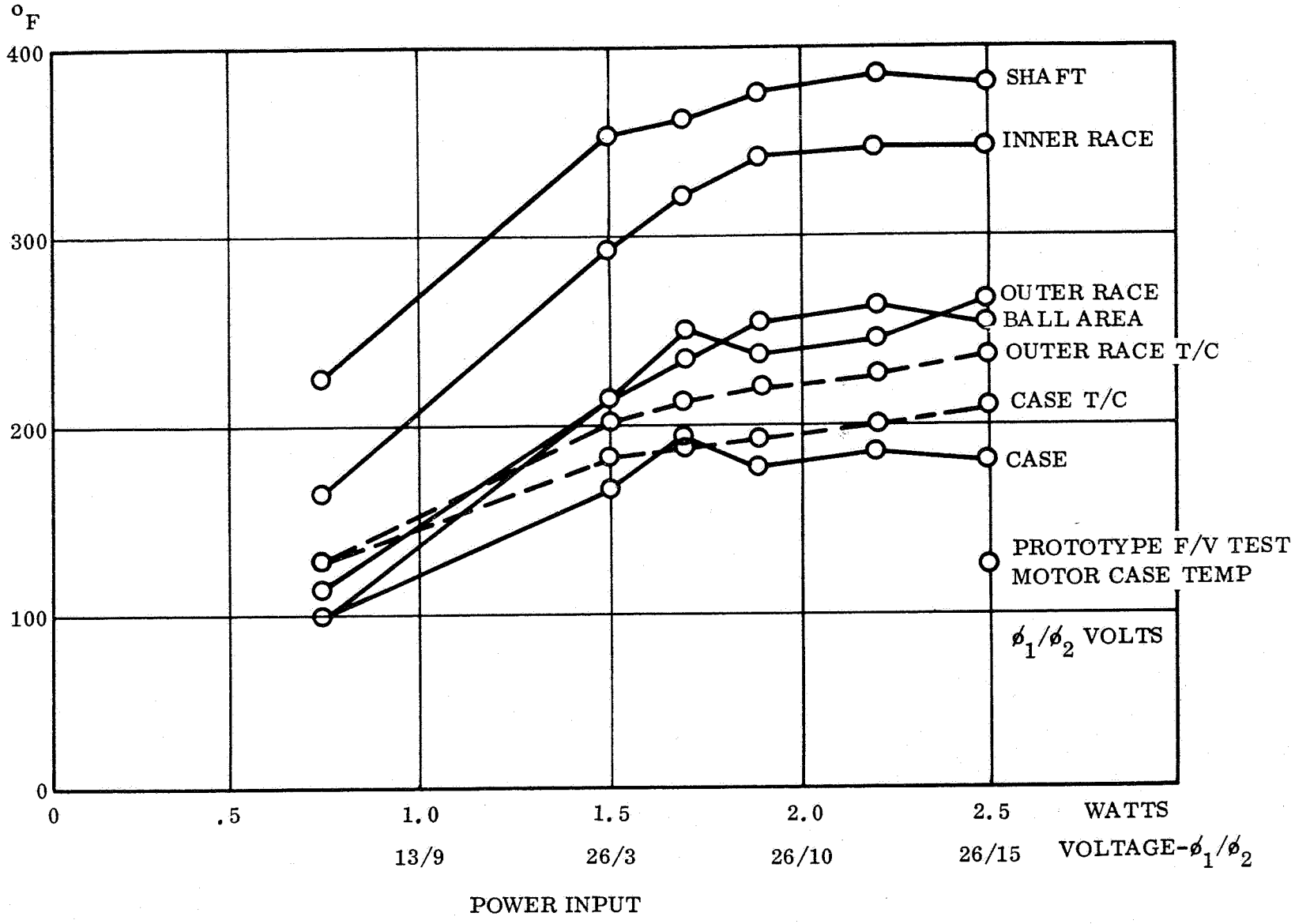

Section 4, Figure 4
Temperature Profile Test Size 8 MGH - Vacuum

5.0 DESIGN IMPROVEMENTS

For future Nimbus vehicles, the Solar Array Drive design has been improved by several key design changes and a larger number of minor revisions. Figures 1 and 2 show the new drive configuration. Figure 3 shows the results of temperature profile tests conducted in the new configuration. Comparing these results with Figure 4 of Section 4, it can be seen that the maximum temperature of the motor rotor has been significantly reduced and that the rotor temperature now runs only slightly above the temperature of the stationary parts of the motor.

The primary improvements were (a) change from a size 8 to a size 11 servo motor, increasing available motor torque. In addition, the motor rotor was coated with high emissivity paint, which together with the increased rotor length gives an order of magnitude improvement for rotor heat rejection over the previous configuration. (b) lowered fixed phase voltage from 26 volts to 10 volts, resulting in approximately four-to-one reduction in input power. (The voltage can be increased to 26 volts by ground command, if necessary). (c) instituted a 100-hour vacuum test with 100 percent teardown and inspection prior to final assembly of the motor gearhead. This procedure revealed several defects in design and quality control which could have caused flight problems.

Other changes of interest are itemized below:

Design

Motor Ball Bearing clearance increased to .0008-.011 inches

Increased motor rotor-stator air gap to .002 inches, minimum (increases contaminant tolerance, lowers rotor heat.)

Sealed rear end of motor

Mounted temperature indicator on motor case end, to be telemetered in flight.

High conductivity heat strap between motor casing and vehicle temperature sink.

Motor mounting to gearhead concentricity improved (eliminated intermediate piece).

Gearhead mounting to drive housing improved (flanged connection).

All flange interfaces greased to promote heat conduction, retard evaporation.

New gearhead gear material (4340), through-hardened and shot-peened.

Ribbon retainers in all ball bearings.

High torque gearhead gears and shafts made of one piece.

Wire splices reduced.

All ball bearings shielded. Motor bearings double-shielded.

Gearhead gears redesigned for greater strength.

Replaced spring separators with phenolic separators on large shaft bearings.

Made output shaft and gear one piece and changed material to nitralloy.

Changed motor-gearhead output gear material to nitralloy; gear now installed by motor gearhead vendor.

Increased quantity of grease

Lockwiring now required.

Separate electrical connectors for potentiometer and drive motor to simplify wire harness.

Replaced snap ring on shaft pin with lock nut.

Changed venting path to minimize air flow through the paddle shaft bearings.

Quality Control

Particulate contaminant and shelf age control of G-300 grease.

Assembly performed only in clean hood.

Instituted complete manufacturing flow plan with inspection points.

Instituted detailed heat treatment procedures, new fixtures to hold parts.

Instituted better control of bearing shaft and housing fits.

Instituted standardized ball bearing grease fill procedure with quantity control.

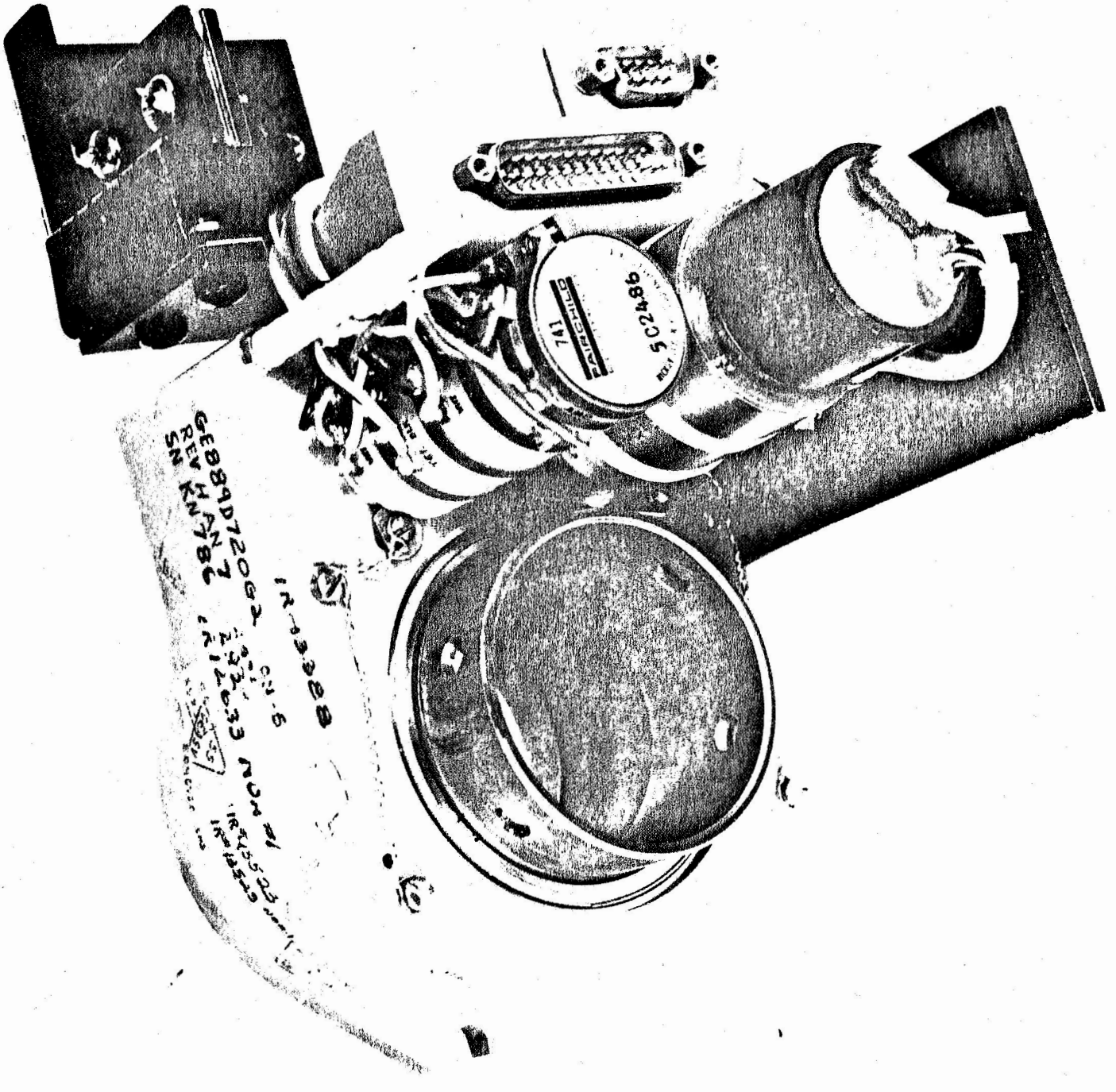

Section 5 - Figure 1
Nimbus II Solar Array Drive

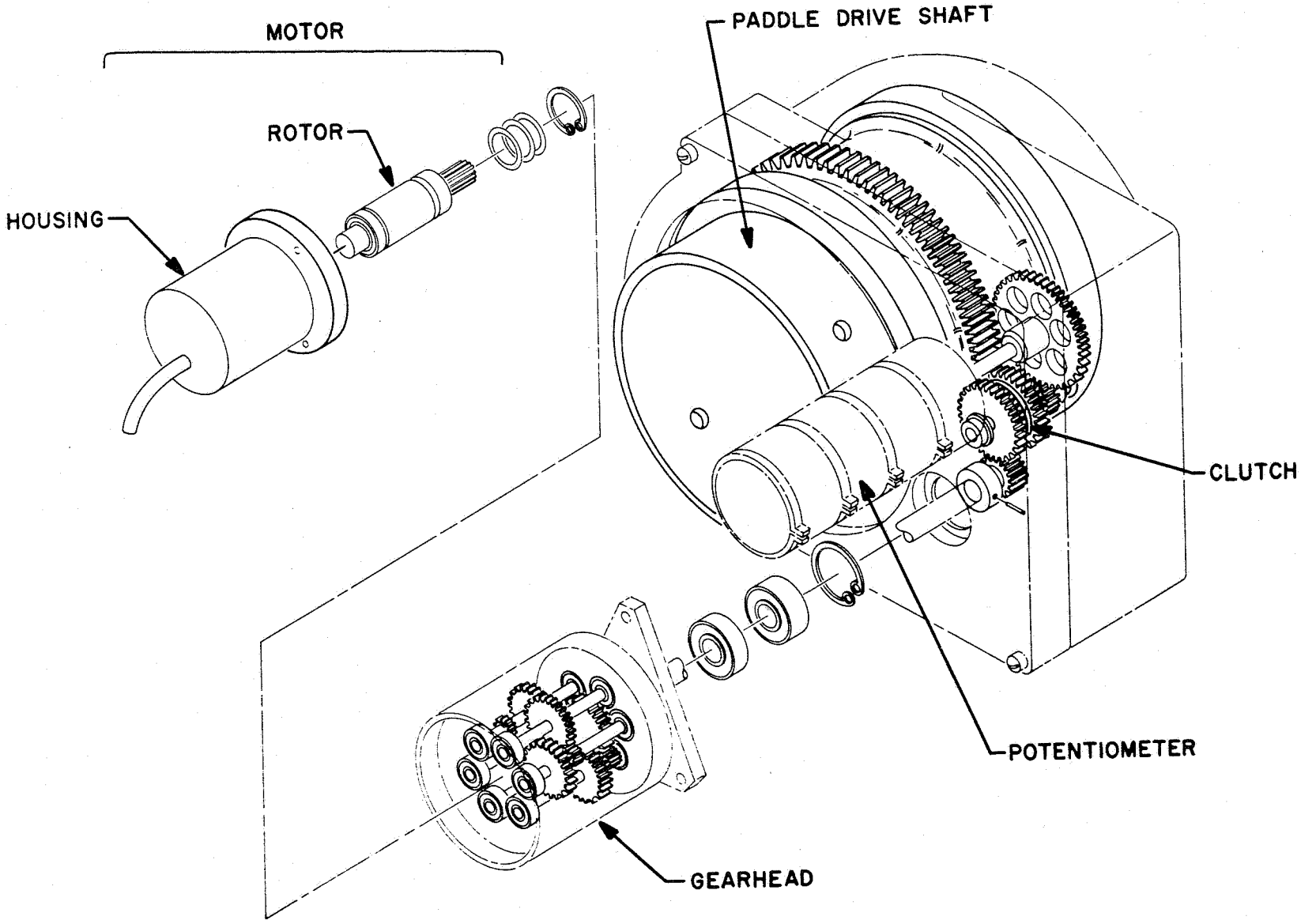

Section 5, Figure 2
Nimbus II Solar Array Drive - Exploded View

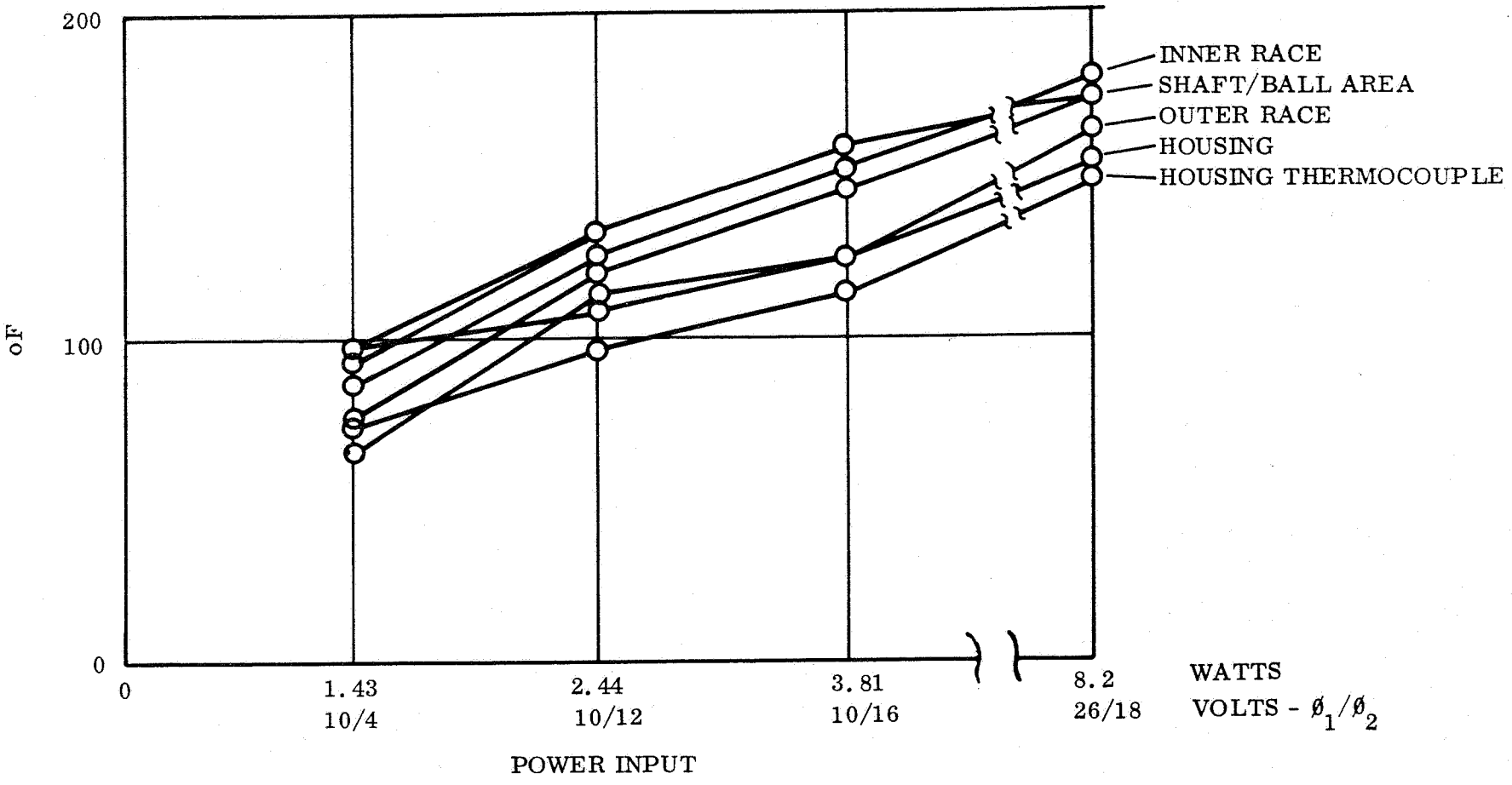

Section 5, Figure 3
Temperature Profile Test Size 11 AC MGH - Vacuum

6.0 LIFE ASSURANCE TESTING

To demonstrate that the new, improved Solar Array Drive design had resolved the previous problems and would perform as required in flight, a life assurance test program was established. The objective of the program was to demonstrate design adequacy for a six-month mission by testing at an accelerated rate in order to obtain a high degree of assurance as soon as possible. A secondary objective was to establish the actual life and wear-out characteristics of the redesigned unit.

For these purposes, a motor gearhead unit and a complete Solar Array Drive unit were placed on life test. To accelerate the test results, an approximation of the dynamic operation of the units during a flight orbit was established as a duty cycle, with the non-operating and steady-state operating portions of the flight orbit reduced. Thus, each test "orbit" was accomplished in approximately 16 minutes as approximately 107 minutes for an actual orbit. In addition, the units were operated at a base-plate temperature of 50 C, corresponding to the anticipated maximum normal temperature expected in flight. The vacuum was maintained at 10^{-6} Torr or better by a diffusion-pumped test chamber.

After 2500 "orbits", corresponding to one mission equivalent in dynamic operations, the test duty cycle was changed to correspond closely to flight orbit operation and accumulate "real time" life data.

As of July 1, 1966, the motor gearhead has accumulated over 6000 hours and 6600 simulated "orbits"; the Solar Array Drive unit has accumulated over 4000 hours and 4400 simulated orbits. The units were partially disassembled and optically inspected after 6000 and 4000 hours respectively. Neither unit showed signs of distress and both are operating normally. The life tests are still proceeding.